TUNEL/TRAP Staining

The TUNEL method was performed using the ApopTag Fluorescein In Situ Apoptosis Detection Kit (CHEMICON international) according to the manufacturer's instructions with a slight modification. This was followed by TRAP staining as previously reported (Kobayashi et al., 2000).

Cytokine Assays

Bone marrow and blood were collected at 2 weeks after sham operation or ovariectomy. Bone-marrow cells were cultured for 3 days in DMEM. The levels of TNFα, IL-1α, and IL-6 in the culture media and serum RANKL were determined by ELISA (R&D Systems).

Western Blot

Osteoclast precursor cells were treated with or without 100 ng/ml of soluble RANKL. After 15 minutes, cell extracts were harvested from the cells using lysis buffer containing 100 mM Tris-HCl (pH 7.8), 150 mM NaCl, 0.1% Triton X-100, 5% protease inhibitor cocktail (Sigma), and 5% phosphatase inhibitor cocktail (Sigma). An equivalent amount of protein from each of the cell extracts and proteins of femoral bone extracted using ISOGEN was loaded for SDS-PAGE and transferred to PVDF membranes (Amersham Biosciences). The membranes were developed with enhanced chemiluminescence reagent (Amersham Biosciences) (Ohtake et al., 2003). Phosphorylation of p38 MAPK and IκB were evaluated using antibodies purchased from Cell Signaling Technology (Koga et al., 2004) and anti-FasL antibody was purchased from Santa Cruz Biotechnology (sc-834).

Actin-Ring Formation

Cells were fixed for 15 min in warm 4% paraformaldehyde (PFA). After fixation, cells were washed three times with PBS with 0.1% Triton X-100 (PBST) and incubated with 0.2 U/ml rhodamine phalloidin (Molecular Probes) for 30 min and washed again three times in PBST.

Statistical Analysis

Data were analyzed by two-tailed student's t test. For all graphs, data are represented as mean ± SEM.

Supplemental Data

Supplemental Data include Supplemental Experimental Procedures and four figures and can be found with this article online at http://www.cell.com/cgi/content/full/130/5/811/DC1/.

ACKNOWLEDGMENTS

We thank Drs. S. Krum and M. Brown to share with their unpublished results; Drs. K. Yoshimura, Y. Nakamichi, T. Watanabe, J. Miyamoto, H. Shiina, T. Fukuda, Ms. Y. Sato, and S. Tanaka for generation of the KO mice; Drs. T. Koga, H. Takagi, E. Ochiai, and N. Moriyama for technical help; Dr. J. Miyazaki for *CAG-CAT-Z* reporter mice, and H. Higuchi and K. Hiraga for manuscript preparation. This work was supported in part by priority areas from the Ministry of Education, Culture, Sports, Science and Technology (to S.K.) and the Program for Promotion of Basic Research Activities for Innovative Biosciences (PROBRAIN).

Received: February 23, 2007
Revised: May 21, 2007
Accepted: July 17, 2007
Published: September 6, 2007

REFERENCES

Belandia, B., and Parker, M.G. (2003). Nuclear receptors: a rendezvous for chromatin remodeling factors. Cell *114*, 277–280.

Bland, R. (2000). Steroid hormone receptor expression and action in bone. Clin. Sci. (Lond.) *98*, 217–240.

Carroll, J.S., Liu, X.S., Brodsky, A.S., Li, W., Meyer, C.A., Szary, A.J., Eeckhoute, J., Shao, W., Hestermann, E.V., Geistlinger, T.R., et al. (2005). Chromosome-wide mapping of estrogen receptor binding reveals long-range regulation requiring the forkhead protein FoxA1. Cell *122*, 33–43.

Chien, K.R., and Karsenty, G. (2005). Longevity and lineages: toward the integrative biology of degenerative diseases in heart, muscle, and bone. Cell *120*, 533–544.

Copeland, N.G., Jenkins, N.A., and Court, D.L. (2001). Recombineering: a powerful new tool for mouse functional genomics. Nat. Rev. Genet. *2*, 769–779.

Couse, J.F., and Korach, K.S. (1999). Estrogen receptor null mice: what have we learned and where will they lead us? Endocr. Rev. *20*, 358–417.

Delmas, P.D. (2002). Treatment of postmenopausal osteoporosis. Lancet *359*, 2018–2026.

Dupont, S., Krust, A., Gansmuller, A., Dierich, A., Chambon, P., and Mark, M. (2000). Effect of single and compound knockouts of estrogen receptors alpha (ERalpha) and beta (ERbeta) on mouse reproductive phenotypes. Development *127*, 4277–4291.

Gowen, M., Lazner, F., Dodds, R., Kapadia, R., Feild, J., Tavaria, M., Bertoncello, I., Drake, F., Zavarselk, S., Tellis, I., et al. (1999). Cathepsin K knockout mice develop osteopetrosis due to a deficit in matrix degradation but not demineralization. J. Bone Miner. Res. *14*, 1654–1663.

Harada, S., and Rodan, G.A. (2003). Control of osteoblast function and regulation of bone mass. Nature *423*, 349–355.

Kameda, T., Mano, H., Yuasa, T., Mori, Y., Miyazawa, K., Shiokawa, M., Nakamaru, Y., Hiroi, E., Hiura, K., Kameda, A., et al. (1997). Estrogen inhibits bone resorption by directly inducing apoptosis of the bone-resorbing osteoclasts. J. Exp. Med. *186*, 489–495.

Karsenty, G. (2006). Convergence between bone and energy homeostases: leptin regulation of bone mass. Cell Metab. *4*, 341–348.

Karsenty, G., and Wagner, E.F. (2002). Reaching a genetic and molecular understanding of skeletal development. Dev. Cell *2*, 389–406.

Kato, S., Ito, S., Noguchi, T., and Naito, H. (1989). Effects of brefeldin A on the synthesis and secretion of egg white proteins in primary cultured oviduct cells of laying Japanese quail (Coturnix coturnix japonica). Biochim. Biophys. Acta *991*, 36–43.

Kawano, H., Sato, T., Yamada, T., Matsumoto, T., Sekine, K., Watanabe, T., Nakamura, T., Fukuda, T., Yoshimura, K., Yoshizawa, T., et al. (2003). Suppressive function of androgen receptor in bone resorption. Proc. Natl. Acad. Sci. USA *100*, 9416–9421.

Kimble, R.B., Matayoshi, A.B., Vannice, J.L., Kung, V.T., Williams, C., and Pacifici, R. (1995). Simultaneous block of interleukin-1 and tumor necrosis factor is required to completely prevent bone loss in the early postovariectomy period. Endocrinology *136*, 3054–3061.

Kobayashi, Y., Hashimoto, F., Miyamoto, H., Kanaoka, K., Miyazaki-Kawashita, Y., Nakashima, T., Shibata, M., Kobayashi, K., Kato, Y., and Sakai, H. (2000). Force-induced osteoclast apoptosis in vivo is accompanied by elevation in transforming growth factor beta and osteoprotegerin expression. J. Bone Miner. Res. *15*, 1924–1934.

Koga, T., Inui, M., Inoue, K., Kim, S., Suematsu, A., Kobayashi, E., Iwata, T., Ohnishi, H., Matozaki, T., Kodama, T., et al. (2004). Costimulatory signals mediated by the ITAM motif cooperate with RANKL for bone homeostasis. Nature *428*, 758–763.

Li, C.Y., Jepsen, K.J., Majeska, R.J., Zhang, J., Ni, R., Gelb, B.D., and Schaffler, M.B. (2006). Mice lacking Cathepsin K maintain bone remodeling but develop bone fragility despite high bone mass. J. Bone Miner. Res. *21*, 865–875.

Mangelsdorf, D.J., Thummel, C., Beato, M., Herrlich, P., Schutz, G., Umesono, K., Blumberg, B., Kastner, P., Mark, M., Chambon, P., and Evans, R.M. (1995). The nuclear receptor superfamily: the second decade. Cell *83*, 835–839.

Martin, T.J., and Sims, N.A. (2005). Osteoclast-derived activity in the coupling of bone formation to resorption. Trends Mol. Med. *11*, 76–81.

Mueller, S.O., and Korach, K.S. (2001). Estrogen receptors and endocrine diseases: lessons from estrogen receptor knockout mice. Curr. Opin. Pharmacol. *1*, 613–619.

Mundy, G.R., and Elefteriou, F. (2006). Boning up on ephrin signaling. Cell *126*, 441–443.

Nakamichi, Y., Shukunami, C., Yamada, T., Aihara, K., Kawano, H., Sato, T., Nishizaki, Y., Yamamoto, Y., Shindo, M., Yoshimura, K., et al. (2003). Chondromodulin I is a bone remodeling factor. Mol. Cell. Biol. *23*, 636–644.

Ohtake, F., Takeyama, K., Matsumoto, T., Kitagawa, H., Yamamoto, Y., Nohara, K., Tohyama, C., Krust, A., Mimura, J., Chambon, P., et al. (2003). Modulation of oestrogen receptor signalling by association with the activated dioxin receptor. Nature *423*, 545–550.

Raisz, L.G. (2005). Pathogenesis of osteoporosis: concepts, conflicts, and prospects. J. Clin. Invest. *115*, 3318–3325.

Riggs, B.L., and Hartmann, L.C. (2003). Selective estrogen-receptor modulators–mechanisms of action and application to clinical practice. N. Engl. J. Med. *348*, 618–629.

Rodan, G.A., and Martin, T.J. (2000). Therapeutic approaches to bone diseases. Science *289*, 1508–1514.

Saftig, P., Hunziker, E., Wehmeyer, O., Jones, S., Boyde, A., Rommerskirch, W., Moritz, J.D., Schu, P., and von Figura, K. (1998). Impaired osteoclastic bone resorption leads to osteopetrosis in Cathepsin-K-deficient mice. Proc. Natl. Acad. Sci. USA *95*, 13453–13458.

Sakai, K., and Miyazaki, J. (1997). A transgenic mouse line that retains Cre recombinase activity in mature oocytes irrespective of the cre transgene transmission. Biochem. Biophys. Res. Commun. *237*, 318–324.

Sato, T., Matsumoto, T., Kawano, H., Watanabe, T., Uematsu, Y., Sekine, K., Fukuda, T., Aihara, K., Krust, A., Yamada, T., et al. (2004). Brain masculinization requires androgen receptor function. Proc. Natl. Acad. Sci. USA *101*, 1673–1678.

Shang, Y., and Brown, M. (2002). Molecular determinants for the tissue specificity of SERMs. Science *295*, 2465–2468.

Shiina, H., Matsumoto, T., Sato, T., Igarashi, K., Miyamoto, J., Takemasa, S., Sakari, M., Takada, I., Nakamura, T., Metzger, D., et al. (2006). Premature ovarian failure in androgen receptor-deficient mice. Proc. Natl. Acad. Sci. USA *103*, 224–229.

Simpson, E.R., and Davis, S.R. (2001). Minireview: aromatase and the regulation of estrogen biosynthesis–some new perspectives. Endocrinology *142*, 4589–4594.

Sims, N.A., Clement-Lacroix, P., Minet, D., Fraslon-Vanhulle, C., Gaillard-Kelly, M., Resche-Rigon, M., and Baron, R. (2003). A functional androgen receptor is not sufficient to allow estradiol to protect bone after gonadectomy in estradiol receptor-deficient mice. J. Clin. Invest. *111*, 1319–1327.

Smith, E.P., Boyd, J., Frank, G.R., Takahashi, H., Cohen, R.M., Specker, B., Williams, T.C., Lubahn, D.B., and Korach, K.S. (1994). Estrogen resistance caused by a mutation in the estrogen-receptor gene in a man. N. Engl. J. Med. *331*, 1056–1061.

Sun, L., Peng, Y., Sharrow, A.C., Iqbal, J., Zhang, Z., Papachristou, D.J., Zaidi, S., Zhu, L.L., Yaroslavskiy, B.B., Zhou, H., et al. (2006). FSH directly regulates bone mass. Cell *125*, 247–260.

Suzawa, M., Takada, I., Yanagisawa, J., Ohtake, F., Ogawa, S., Yamauchi, T., Kadowaki, T., Takeuchi, Y., Shibuya, H., Gotoh, Y., et al. (2003). Cytokines suppress adipogenesis and PPAR-gamma function through the TAK1/TAB1/NIK cascade. Nat. Cell Biol. *5*, 224–230.

Syed, F., and Khosla, S. (2005). Mechanisms of sex steroid effects on bone. Biochem. Biophys. Res. Commun. *328*, 688–696.

Takeda, S., Elefteriou, F., Levasseur, R., Liu, X., Zhao, L., Parker, K.L., Armstrong, D., Ducy, P., and Karsenty, G. (2002). Leptin regulates bone formation via the sympathetic nervous system. Cell *111*, 305–317.

Takezawa, S., Yokoyama, A., Okada, M., Fujiki, R., Iriyama, A., Yanagi, Y., Ito, H., Takada, I., Kishimoto, M., Miyajima, A., et al. (2007). A cell cycle-dependent co-repressor mediates photoreceptor cell-specific nuclear receptor function. EMBO J. *26*, 764–774.

Teitelbaum, S.L. (2006). Osteoclasts: culprits in inflammatory osteolysis. Arthritis Res. Ther. *8*, 201.

Teitelbaum, S.L. (2007). Osteoclasts: what do they do and how do they do it? Am. J. Pathol. *170*, 427–435.

Teitelbaum, S.L., and Ross, F.P. (2003). Genetic regulation of osteoclast development and function. Nat. Rev. Genet. *4*, 638–649.

Tolar, J., Teitelbaum, S.L., and Orchard, P.J. (2004). Osteopetrosis. N. Engl. J. Med. *351*, 2839–2849.

Windahl, S.H., Andersson, G., and Gustafsson, J.A. (2002). Elucidation of estrogen receptor function in bone with the use of mouse models. Trends Endocrinol. Metab. *13*, 195–200.

Yoshizawa, T., Handa, Y., Uematsu, Y., Takeda, S., Sekine, K., Yoshihara, Y., Kawakami, T., Arioka, K., Sato, H., Uchiyama, Y., et al. (1997). Mice lacking the vitamin D receptor exhibit impaired bone formation, uterine hypoplasia and growth retardation after weaning. Nat. Genet. *16*, 391–396.

Zaman, G., Jessop, H.L., Muzylak, M., De Souza, R.L., Pitsillides, A.A., Price, J.S., and Lanyon, L.L. (2006). Osteocytes use estrogen receptor alpha to respond to strain but their ERalpha content is regulated by estrogen. J. Bone Miner. Res. *21*, 1297–1306.

Accession Numbers

Microarray can be seen in Gene Expression Omnibus under accession number GSE7798.

0090-9556/07/3510-1949–1955$20.00
DRUG METABOLISM AND DISPOSITION
Copyright © 2007 by The American Society for Pharmacology and Experimental Therapeutics
DMD 35:1949–1955, 2007

Vol. 35, No. 10
17327/3255799
Printed in U.S.A.

A Novel Mechanism for Polychlorinated Biphenyl-Induced Decrease in Serum Thyroxine Level in Rats

Yoshihisa Kato, Shin-ichi Ikushiro, Rie Takiguchi, Koichi Haraguchi, Nobuyuki Koga, Shinya Uchida, Toshiyuki Sakaki, Shizuo Yamada, Jun Kanno, and Masakuni Degawa

Kagawa School of Pharmaceutical Sciences, Tokushima Bunri University, Sanuki, Kagawa, Japan (Y.K.); Faculty of Engineering, Toyama Prefectural University, Toyama, Japan (S.I., T.S.); School of Pharmaceutical Sciences and Center of Excellence (COE) Program in the 21st Century, University of Shizuoka, Shizuoka, Japan (R.T., S.U., S.Y., M.D.); Daiichi College of Pharmaceutical Sciences, Fukuoka, Japan (K.H.); Faculty of Nutritional Sciences, Nakamura Gakuen University, Fukuoka, Japan (N.K.); and Division of Cellular & Molecular Toxicology, National Institute of Health Sciences, Tokyo, Japan (J.K.)

Received June 19, 2007; accepted July 12, 2007

ABSTRACT:

We have previously suggested that the decrease in the levels of serum total thyroxine (T_4) and free T_4 by a single administration to rats of Kanechlor-500 (KC500) at a dose of 100 mg/kg is not necessarily dependent on the increase in hepatic T_4-UDP-glucuronosyltransferase (UDP-GT). In the present study, we determined whether or not a consecutive treatment with KC500 at a relatively low dose (10 mg/kg i.p., once daily for 10 days) results in a decrease in the level of serum total T_4 and further investigated an exact mechanism for the KC500-induced decrease in the T_4. At 4 days after final treatment with KC500, the serum total T_4 and free T_4 levels were markedly decreased in both Wistar and UGT1A-deficient Wistar (Gunn) rats, whereas significant increases in hepatic T_4-UDP-GT activity were observed in Wistar rats but not in Gunn rats. The level of serum thyroid-stimulating hormone was not significantly changed in either Wistar or Gunn rats. Clearance from serum of the [^{125}I]T_4 administered to the KC500-pretreated Wistar and Gunn rats was faster than that to the corresponding control (KC500-untreated) rats. The accumulated level of [^{125}I]T_4 was increased in several tissues, especially the liver, in the KC500-pretreated rats. The present findings demonstrated that a consecutive treatment with KC500 resulted in a significant decrease in the level of serum total T_4 in both Wistar and Gunn rats and further indicated that the KC500-induced decrease would occur through increase in accumulation of T_4 in several tissues, especially the liver, rather than increase in hepatic T_4-UDP-GT activity.

Most polychlorinated biphenyls (PCBs) are known to decrease the level of serum thyroid hormone and to increase the activity of hepatic drug-metabolizing enzymes in rats (Van Birgelen et al., 1995; Craft et al., 2002). As possible mechanisms for the PCB-induced decrease in the level of serum thyroid hormone, enhancement of thyroid hormone metabolism by PCB and displacement of the hormone from serum transport proteins, including transthyretin (TTR), by PCB and its ring-hydroxylated metabolites are considered (Barter and Klaassen, 1992a, 1994; Brouwer et al., 1998). In particular, the decrease in the level of serum thyroxine (T_4) by 3,3′,4,4′,5-pentachlorobiphenyl, Aroclor 1254, and 2,3,7,8-tetrachlorodibenzo-*p*-dioxin in rats is believed to occur mainly through induction of the UDP-glucuronosyltransferases (UDP-GTs), especially UGT1A subfamily enzymes, responsible for glucuronidation of T_4 (Barter and Klaassen, 1994; Van Birgelen et al., 1995). However, the magnitude of decrease in the level of serum total T_4 is not necessarily correlated with that of increase in T_4-UDP-GT activity (Craft et al., 2002; Hood et al., 2003). Furthermore, we have reported that in Kanechlor-500 (KC500)-treated mice, serum T_4 level decreased without an increase in T_4-UDP-GT activity (Kato et al., 2003) and that the decrease in serum total T_4 level by a single administration of either KC500 or 2,2′,4,5,5′-pentachlorobiphenyl occurred even in UGT1A-deficient Wistar (Gunn) rats (Kato et al., 2004). Thus, an exact mechanism for the PCB-induced decrease in the level of serum thyroid hormone remains unclear. To date, most studies on biological effects of PCB have been performed using experimental animals treated once at a high dose (more than 100 mg/kg body weight), and the effect of the consecutive treatment at a low dose has been little reported. Humans and wild animals are exposed to a wide variety of environmental chemicals, including PCB, at a low level over a long period of time. Therefore, a study on biological effects by consecutive treatment with PCB at a low dose would be very important.

In the present study, therefore, we examined whether or not a consecutive treatment with KC500 at a relatively low dose (10 mg/kg i.p., once daily for 10 days) results in decrease in the level of serum total T_4 and further discussed a mechanism underlying the PCB-induced decrease in the T_4.

This work was supported in part by the Grant-in-Aid for Scientific Research (C) (no. 18510061; Y.K.) and for Scientific Research (B) (no. 19310042; K.H., Y.K.) from Japan Society for the Promotion of Science, and by a Health and Labour Sciences Research Grant for Research on Risk of Chemical Substances (H16-Kagaku-003; Y.K.) from the Ministry of Health, Labour and Welfare of Japan.

Article, publication date, and citation information can be found at http://dmd.aspetjournals.org.

doi:10.1124/dmd.107.017327.

ABBREVIATIONS: PCB, polychlorinated biphenyl; KC500, Kanechlor-500; T_3, triiodothyronine; T_4, thyroxine; TTR, transthyretin; TSH, thyroid-stimulating hormone; UDP-GT, UDP-glucuronosyltransferase.

Materials and Methods

Chemicals. Panacete 810 (medium-chain triglycerides) was purchased from Nippon Oils and Fats Co. Ltd. (Tokyo, Japan). The [^{125}I]T_4, radiolabeled at the 5'-position of the outer ring, was obtained from PerkinElmer Life and Analytical Sciences (Waltham, MA). The KC500 used in the present experiments contains 2,2',5,5'-tetrachlorobiphenyl (5.6% of total PCBs), 2,2',3,5',6-pentachlorobiphenyl (6.5%), 2,2',4,5,5'-pentachlorobiphenyl (10%), 2,3,3',4',6-pentachlorobiphenyl (7.4%), 2,3',4,4',5-pentachlorobiphenyl (7.7%), 2,2',3,4,4',5'-hexachlorobiphenyl (5.6%), and 2,2',4,4',5,5'-hexachlorobiphenyl (5.4%) as major PCB congeners (Haraguchi et al., 2005). All the other chemicals used herein were obtained commercially in appropriate grades of purity.

Animal Treatments. Male Wistar rats (160–200 g) and UGT1A-deficient Wistar rats (Gunn rats, 190–260 g) were obtained from Japan SLC., Inc. (Shizuoka, Japan). Male Wistar and Gunn rats were housed three or four per cage with free access to commercial chow and tap water, maintained on a 12-h dark/light cycle (8:00 AM to 8:00 PM light) in an air-controlled room (temperature, 24.5 ± 1°C; humidity, 55 ± 5%), and handled with human care under the guidelines of the University of Shizuoka (Shizuoka, Japan). Rats received consecutive intraperitoneal injections of KC500 (10 mg/kg) dissolved in Panacete 810 (5 ml/kg) at 24-h intervals for 10 days. Control animals were treated with vehicle alone (5 mg/kg).

In Vivo Study. Rats were killed by decapitation 4 days after the final administration of KC500. The liver was removed, and hepatic microsomes were prepared according to the method of Kato et al. (1995) and stored at −85°C until use. Blood was collected from each animal between 10:30 and 11:30 AM. After clotting at room temperature, serum was separated by centrifugation and stored at −50°C until use.

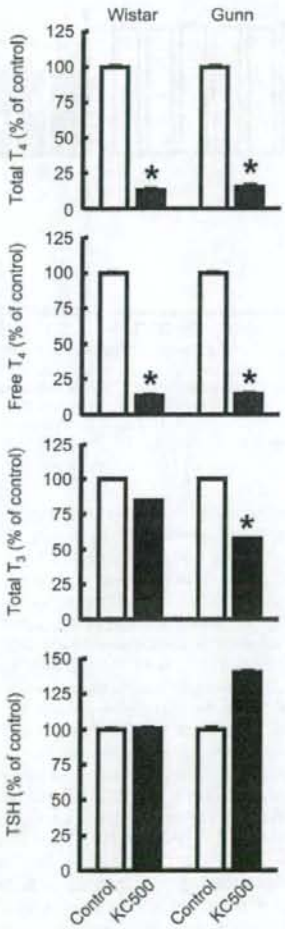

FIG. 1. Effects of KC500 on levels of serum total T_4, free T_4, total T_3, and TSH in Wistar and Gunn rats. Animals were killed 4 days after the final administration of KC500 (10 mg/kg i.p., once daily for 10 days), and levels of serum thyroid hormones were measured as described under *Materials and Methods*. Constitutive levels: total T_4, 4.29 ± 0.38 (Wistar, $n = 5$) and 5.80 ± 0.32 μg/dl (Gunn, $n = 5$); free T_4, 2.17 ± 0.16 (Wistar, $n = 5$) and 2.71 ± 0.17 ng/dl (Gunn, $n = 5$); total T_3, 0.34 ± 0.03 (Wistar, $n = 6$) and 0.96 ± 0.05 ng/ml (Gunn, $n = 4$); TSH, 4.89 ± 0.33 (Wistar, $n = 5$) and 7.48 ± 1.14 ng/ml (Gunn, $n = 5$). Each column represents the mean ± S.E. (vertical bars) for five to six animals. *, $P < 0.01$, significantly different from each control.

TABLE 1

Effects of KC500 on the activity of hepatic microsomal alkoxyresorufin O-dealkylases in Wistar and Gunn rats

Animals were killed at 4 days after the final administration of KC500 (10 mg/kg i.p., once daily for 10 days). The values shown are expressed as the mean ± S.E. for four to five animals.

Substrates	Wistar		Gunn	
	Control	KC500	Control	KC500
	nmol/mg protein/min		*nmol/mg protein/min*	
7-Benzyloxyresorufin	0.07 ± 0.01	3.34 ± 0.33*	0.03 ± 0.003	1.08 ± 0.27*
7-Pentoxyresorufin	0.03 ± 0.003	0.43 ± 0.05*	0.02 ± 0.003	0.22 ± 0.05*
7-Ethoxyresorufin	0.14 ± 0.01	9.02 ± 0.09*	0.21 ± 0.01	2.21 ± 0.29*

* $P < 0.05$, significantly different from each control.

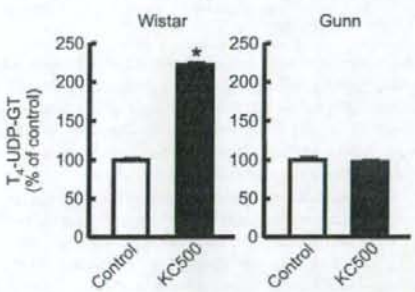

FIG. 2. Effects of KC500 on the activity of hepatic microsomal UDP-glucuronyltransferase in Wistar and Gunn rats. Each column represents the mean ± S.E. (vertical bars) for five to six animals. Constitutive levels: T_4-UDP-GT, 14.17 ± 1.11 pmol/mg protein/min (Wistar) and 6.36 ± 1.34 pmol/mg protein/min (Gunn). *, $P < 0.01$, significantly different from each control.

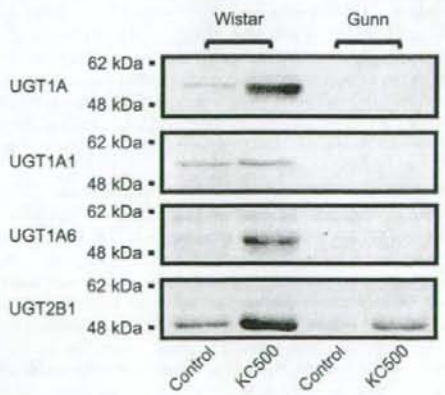

FIG. 3. Representative Western blot profiles for hepatic microsomal UGT isoforms in the KC500-treated Wistar and Gunn rats.

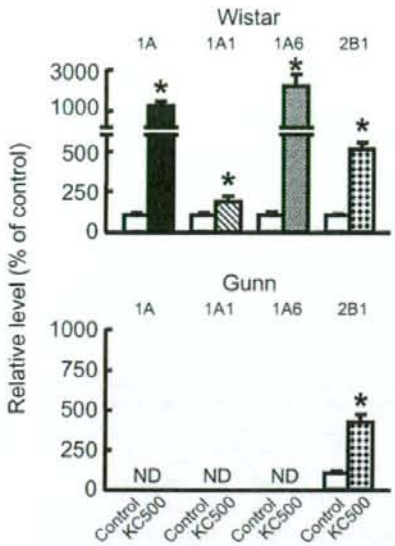

FIG. 4. Effects of KC500 on levels of hepatic microsomal UGT isoforms in Wistar and Gunn rats. The isolated bands responsible for UGT isoforms, which are shown in Fig. 3, were densitometrically quantified as described under *Materials and Methods*. The data are represented as the mean ± S.E. (vertical bars) for five to six animals. *, $P < 0.05$, significantly different from each control. ND, not detectable.

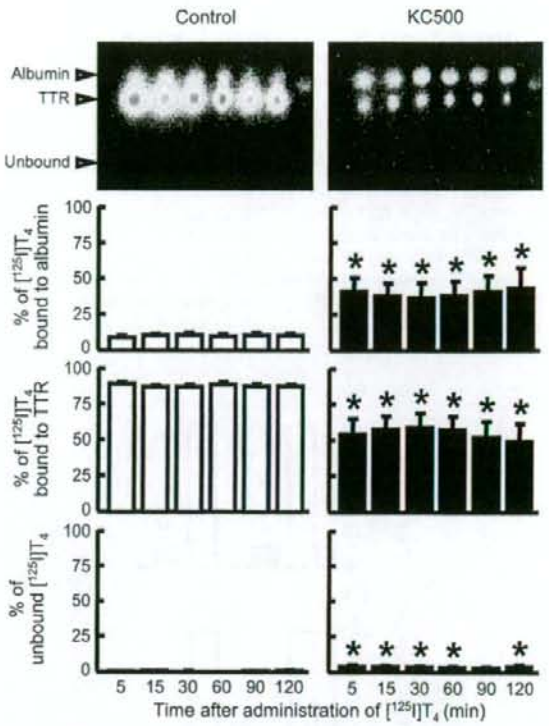

FIG. 5. Effects of KC500 on the binding of $[^{125}I]T_4$ to serum proteins in Wistar rats. Amounts of $[^{125}I]T_4$ bound to the serum proteins were assessed by the method described under *Materials and Methods*. Each column represents the mean ± S.E. (vertical bars) for three to six animals. *, $P < 0.05$, significantly different from each control.

Analysis of serum hormones. Levels of total T_4, free T_4, total triiodothyronine (T_3), and thyroid-stimulating hormone (TSH) were measured by radioimmunoassay using Total T4 and Free T4 kits (Diagnostic Products Corporation, Los Angels, CA), the Triiodothyronine kit GammaCoat T_3 II (DiaSorin Inc., Stillwater, MN), and the rTSH $[^{125}I]$ Biotrak assay system (GE Healthcare UK, Ltd., Little Chalfont, Buckinghamshire, UK), respectively.

Hepatic microsomal enzyme assays. Hepatic microsomal fraction was prepared according to the method described previously (Kato et al., 1995), and the amount of hepatic microsomal protein was determined by the method of Lowry et al. (1951) with bovine serum albumin as a standard. Microsomal *O*-dealkylase activities of 7-benzyloxy-, 7-ethoxy-, and 7-pentoxyresorufins were determined by the method of Burke et al. (1985).

Hepatic T_4-metabolizing enzyme assay. The activity of microsomal UDP-GT toward T_4 (T_4-UGT activity) was determined by the methods of Barter and Klaassen (1992b).

Western blot analysis. The polyclonal anti-peptide antibodies against the common region of UGT1A isoforms and specific antibodies against UGT1A1, UGT1A6, and UGT2B1, which were established by Ikushiro et al. (1995, 1997), were used. Western blot analyses for microsomal UGT isoforms were performed by the method of Luquita et al. (2001). The bands corresponding to UGT1A1, UGT1A6, and UGT2B1 on a sheet were detected using chemical luminescence (ECL detection kit; GE Healthcare UK, Ltd.), and the level of each protein was determined densitometrically with LAS-1000 (Fuji Photo Film. Co., Ltd., Tokyo, Japan).

Ex Vivo Study. At 4 days after a consecutive 10-day treatment with KC500, the rats were anesthetized with a saline (2 ml/kg) containing sodium pentobarbital (25 mg/ml) and potassium iodide (1 mg/ml). The femoral artery was cannulated (polyethylene tube SP31; Natsume Inc., Tokyo, Japan) and primed with heparinized saline (33 units/ml), and then the animal's body was warmed to 37°C. Fifteen minutes later, the rats were given i.v. 1 ml of $[^{125}I]T_4$ (15 μCi /ml) dissolved in the saline containing 10 mM NaOH and 1% normal rat serum.

Clearance of $[^{125}I]T_4$ from serum. The study on the clearance of $[^{125}I]T_4$ from serum was performed according to the method of Oppenheimer et al. (1968). In brief, after the administration of $[^{125}I]T_4$, a portion (0.3 ml) of blood was sampled from the artery at the indicated times, and serum was prepared and stored at −50°C until use. Two aliquots (15 μl each) were taken from each serum sample for determining $[^{125}I]T_4$ level by a gamma counter (COBRA II AUTO-GAMMA 5002; PerkinElmer Life and Analytical Sciences).

Analysis of $[^{125}I]T_4$ bound to serum proteins. The levels of serum $[^{125}I]T_4$-albumin and $[^{125}I]T_4$-TTR complexes were determined according to the method of Davis et al. (1970). In brief, serum was diluted in 100 mM phosphate buffer (pH 7.4) containing 1 mM EDTA, 1 mM dithiothreitol, and 30% glycerol, and subjected to electrophoresis on 4 to 20% gradient native polyacrylamide gels PAG Mid "Daiichi" 4/20 (Daiichi Pure Chemicals Co., Ltd., Tokyo, Japan). The electrophoresis was performed at 4°C for 11 h at 20 mA in the 0.025 M Tris buffer (pH 8.4) containing 0.192 M glycine. The human albumin and TTR, which were incubated with $[^{125}I]T_4$, were also applied on the gel as templates. After the electrophoresis, a gel was dried and radioautographed for 20 h at room temperature using Imaging Plate 2040 (Fuji Photo Film Co., Ltd.). The levels of $[^{125}I]T_4$-albumin and $[^{125}I]T_4$-TTR in serum were determined by counting the gel fractions identified from Bio Imaging Analyzer (BAS-2000II IP Reader; Fuji Photo Film Co., Ltd.).

Tissue distribution of $[^{125}I]T_4$. The study on the tissue distribution of $[^{125}I]T_4$ was performed according to the modified method of Oppenheimer et al. (1968). In brief, at 60 min after administration of $[^{125}I]T_4$ to KC500-pretreated rats, blood was sampled from abdominal aorta. Then, cerebrum, cerebellum, pituitary gland, thyroid gland, sublingual gland, submandibular gland, thymus, heart, lung, liver, kidney, adrenal gland, spleen, pancreas, testis, prostate gland, seminal vesicle, stomach, duodenum, jejunum, ileum, cecum, brown fat, skeletal muscle, bone marrow skin, spinal cord, and fat were removed and weighed. Radioactivities in serum and the tissues were determined by a gamma-counter (COBRA II AUTO-GAMMA5002; PerkinElmer Life and Analytical Sciences), and amounts of $[^{125}I]T_4$ in various tissues were shown as ratios of tissue to serum.

Statistics. The data obtained were statistically analyzed according to Stu-

dent's *t* test or Dunnett's test after analysis of variance. In addition, data of the clearance of $[^{125}I]T_4$ from serum and analysis of $[^{125}I]T_4$ bound to serum proteins were statistically analyzed according to the Newman-Keuls test after analysis of variance. The pharmacokinetic parameters of $[^{125}I]T_4$ were estimated with noncompartmental methods as described previously (Tabata et al., 1999).

Results

Serum Hormone Levels. Effects of KC500 on levels of serum thyroid hormones were examined in Wistar and Gunn rats (Fig. 1). In both Wistar and Gunn rats, KC500 treatment resulted in decreases of the serum total T_4 and free T_4, and the magnitude of the decrease in each serum thyroid hormone was almost the same in both strains of rats. On the other hand, a significant decrease in the level of serum total T_3 was observed in Gunn rats but not in Wistar rats. In addition, no significant change in TSH level was observed in either Wistar or Gunn rats.

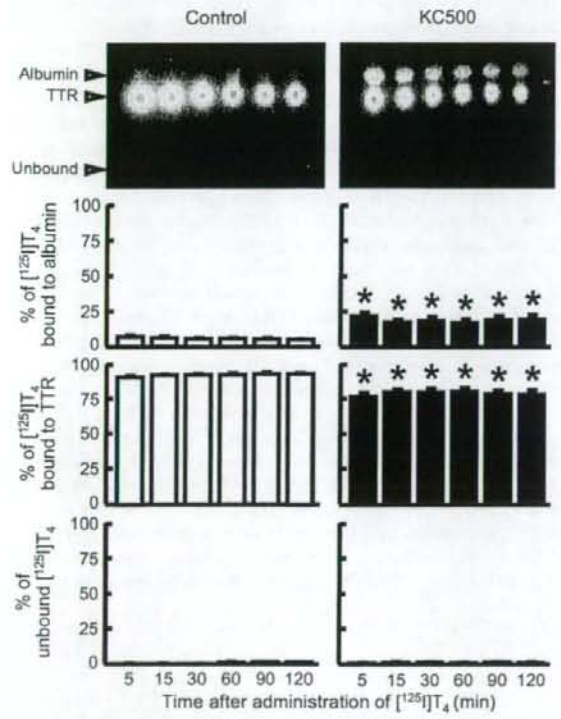

FIG. 6. Effects of KC500 on the binding of $[^{125}I]T_4$ to serum proteins in Gunn rats. Amounts of $[^{125}I]T_4$ bound to the serum proteins were assessed by the method described under *Materials and Methods*. Each column represents the mean ± S.E. (vertical bars) for four to five animals. *, $P < 0.05$, significantly different from each control.

Hepatic Drug-Metabolizing Enzymes. Effects of KC500 on hepatic microsomal activities of benzyloxyresorufin *O*-dealkylase (CYP2B1/2 and CYP3A1/2), pentoxyresorufin *O*-dealkylase (CYP2B1/2), and ethoxyresorufin *O*-dealkylase (CYP1A1/2) were examined in Wistar and Gunn rats. In both Wistar and Gunn rats, these enzyme activities were significantly increased by KC500 (Table 1), and the increase in each enzyme activity was much greater in Wistar rats than in Gunn rats.

Hepatic T_4-Metabolizing Enzyme Activities. T_4 glucuronidation is primarily mediated by hepatic T_4-UDP-GTs, such as UGT1A1 and UGT1A6, in the rat liver (Visser, 1996), and a chemical-mediated induction of the enzymes is considered to contribute to the decrease in the level of serum total T_4. Therefore, we examined effects of KC500 on hepatic microsomal T_4-UDP-GT activity in Wistar and Gunn rats. Constitutive activity of T_4-UDP-GT was approximately 2.2-fold higher in Wistar rats than in Gunn rats. Treatment with KC500 resulted in significant increase of T_4-UDP-GT activity in Wistar rats but not in Gunn rats (Fig. 2).

Western Blot Analysis for UGT1As. Levels of the proteins responsible for UGT1A enzymes, UGT1A1 and UGT1A6, were increased by KC500 treatment in Wistar rats but not in Gunn rats (Figs. 3 and 4). In addition, no expression of the UGT1A enzymes was confirmed in Gunn rats. On the other hand, the level of UGT2B1 was significantly increased by KC500 in both Wistar and Gunn rats, and magnitudes of the increase in both strains of rats were almost the same (Figs. 3 and 4).

Serum Proteins Bound to $[^{125}I]T_4$. The effects of KC500 on the binding of $[^{125}I]T_4$ to serum proteins, TTR, and albumin were examined in Wistar and Gunn rats (Figs. 5 and 6). In both Wistar and Gunn rats, pretreatment with KC500 resulted in a significant decrease in the level of $[^{125}I]T_4$-TTR complex, whereas it resulted in a significant increase in the level of $[^{125}I]T_4$ bound to albumin (Figs. 5 and 6).

Clearance of $[^{125}I]T_4$ from Serum. After an i.v. administration of $[^{125}I]T_4$ to the KC500-pretreated Wistar and Gunn rats, concentrations of $[^{125}I]T_4$ in sera were measured at the indicated times (Fig. 7). In both Wistar and Gunn rats, pretreatment with KC500 promoted the clearance of $[^{125}I]T_4$ from serum, and their serum $[^{125}I]T_4$ levels were decreased to approximately 40% of the initial level within 5 min. In the KC500-untreated Wistar and Gunn rats, serum $[^{125}I]T_4$ levels were gradually decreased to approximately 40% of the initial level at 120 min later. The serum pharmacokinetic parameters of the $[^{125}I]T_4$ estimated from these data (Fig. 7) were summarized in Table 2. The mean total body clearances (CL_{tb}) of $[^{125}I]T_4$ in the KC500-pretreated rats were 2.4 and 2.9 times, respectively, greater than those in the corresponding control rats. The steady-state volumes of distribution (Vd_{ss}) in the KC500-pretreated rats were 1.6 and 2.4 times, respectively, larger than those in the corresponding control rats.

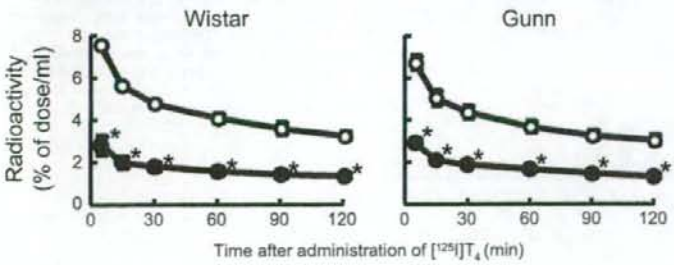

FIG. 7. Effects of KC500 on the clearance of $[^{125}I]T_4$ from serum in Wistar and Gunn rats. The amount of serum $[^{125}I]T_4$ was measured at the indicated times after the i.v. administration of $[^{125}I]T_4$. Each point represents the mean ± S.E. (vertical bars) for four to eight animals. *, $P < 0.001$, significantly different from each control. ○, control; ●, KC500.

Tissue Distribution of [^{125}I]T_4. The tissue-to-serum concentration ratio (K_p value) and distribution level of [^{125}I]T_4 in tissue after the administration of [^{125}I]T_4 to the KC500-pretreated Wistar and Gunn rats are shown in Figs. 8 and 9, respectively. K_p values of the thyroid gland and liver were the greatest among those of the tissues examined in either Wistar or Gunn rats (Fig. 8). In addition, K_p values in all the tissues examined, with the exception of the testis and ileum, were greater in KC500-pretreated Wistar rats than those in the corresponding control (KC500-untreated) rats. K_p values in the thyroid gland, liver, and jejunum in the KC500-pretreated Wistar and Gunn rats were 1.6 to 1.8, 3.3 to 3.8, and 4.7 to 11.5 times, respectively, higher than those in corresponding control rats (Fig. 8).

In the control Wistar and Gunn rats, the accumulation level of [^{125}I]T_4 was highest in the liver, among the tissues examined (Fig. 9). In both Wistar and Gunn rats, pretreatment with KC500 resulted in an increase in the accumulation level in the liver, and the levels increased to more than 40% of the [^{125}I]T_4 dosed (Fig. 9). Likewise, significant increase in accumulation of [^{125}I]T_4 was observed in the jejunum (Fig. 9). In addition, significant increases in the liver weight and accumulation level (per g liver) of [^{125}I]T_4 occurred in KC500-pretreated Wistar rats, but not in Gunn rats (Tables 3 and 4).

Discussion

In the present study, we found that consecutive treatment with KC500 (10 mg/kg i.p., once daily for 10 days; total dose, 100 mg/kg) promoted accumulation of T_4 in several tissues, especially the liver, and resulted in a drastic decrease in the levels of serum total T_4 and free T_4 in both Wistar and Gunn (UGT1A-deficient) rats. Thus, a decrease in the level of serum total T_4 is also observed in the Wistar and Gunn rats treated with KC500 (a single i.p. administration at a dose of 100 mg/kg) (Kato et al., 2004). In addition, constitutive levels of serum total T_4 and T_3 were higher in Gunn rats than in Wistar rats, and the results were identified with those as previously described by Benathan et al. (1983). The difference in constitutive level of serum thyroid hormone between Wistar and Gunn rats seems to be dependent on differences in the level and/or activity of T_4/T_3-UDP-GTs.

As a possible explanation for a chemical-induced decrease in serum thyroid hormones, a hepatic T_4-UDP-GT-dependent mechanism is generally considered, because T_4-UDP-GT inducers, including PCB, phenobarbital, 3-methylcholanthrene, pregnenolone-16α-carbonitrile, and clobazam, show strong activities for decreasing the level of serum total thyroid hormones, including T_4 and T_3 (Barter and Klaassen, 1994; Van Birgelen et al., 1995; Miyawaki et al., 2003). However, among the experimental animals treated with a T_4-UDP-GT inducer, the difference in magnitude of decrease in the level of serum total T_4 is not necessarily correlated with that of hepatic T_4-UDP-GT activity (Craft et al., 2002; Hood et al., 2003; Kato et al., 2003). Our present and previous results (Kato et al., 2004, 2005) using Wistar and Gunn rats support a hypothesis that significant decrease in the level of serum total thyroid hormones by either PCB or phenobarbital occurs primarily in a hepatic T_4-UDP-GT-independent pathway.

As a possible mechanism for the PCB-induced decrease in serum T_4 level, an increase in hepatic drug-metabolizing enzymes might be considered. However, these are induced to a greater extent in the Wistar rats than in the Gunn rats, whereas magnitudes of decrease in serum T_4 level in Wistar and Gunn rats were almost the same. Accordingly, the KC500-induced decrease in serum T_4 level is thought to be independent of the KC500-induced drug-metabolizing enzymes, including UDT-GTs and cytochromes P450.

As the factors regulating the level of serum total T_4, serum TSH, hepatic type I iodothyronine deiodinase, and TTR are known. However, no significant change in the level of serum TSH occurs in the PCB-treated rats (Liu et al., 1995; Hood et al., 1999; Hallgren et al., 2001; Kato et al., 2004). Hepatic type I iodothyronine deiodinase activity was significantly decreased in Wistar and Gunn rats by KC500 (Kato et al., 2004). On the other hand, a TTR-associated pathway might be considered as an explanation for the PCB-induced decrease in the level of serum total

TABLE 2

Pharmacokinetic parameters for [^{125}I]T_4 after the administration of [^{125}I]T_4 to the KC500-pretreated Wistar and Gunn rats

The experimental conditions were the same as those described in Fig. 7. The values shown are expressed as the mean ± S.E. for four to seven animals.

Animal	Treatment	Mean Total Body Clearance × 100	Distribution Volume
		ml/min	*ml*
Wistar	Control	7.82 ± 0.59	17.91 ± 0.52
	KC500	18.85 ± 3.49*	51.51 ± 6.34*
Gunn	Control	8.44 ± 0.22	20.21 ± 1.79
	KC500	13.84 ± 0.88*	48.91 ± 3.50*

* $P < 0.05$, significantly different from each control.

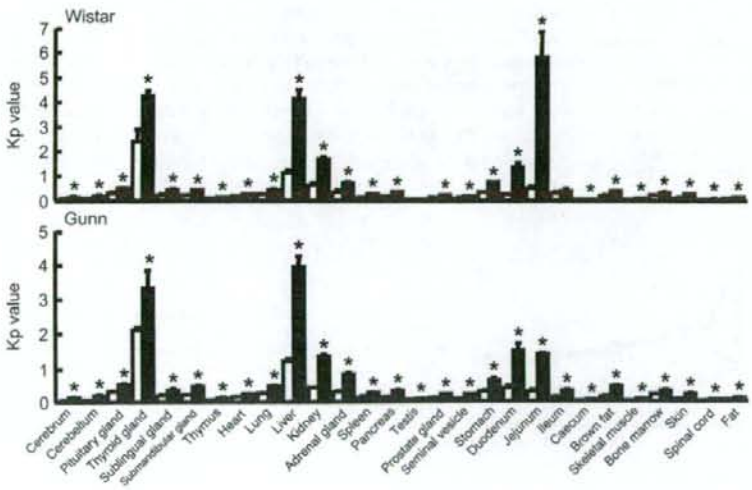

FIG. 8. Tissue-to-serum concentration ratio (K_p value) of [^{125}I]T_4 in various tissues after administration of [^{125}I]T_4 to the KC500-pretreated Wistar and Gunn rats. KC500 (10 mg/kg) was given i.p. to animals once daily for 10 days, and then, the animals were administered i.v. [^{125}I]T_4. At 60 min after administration of [^{125}I]T_4, the radioactivity in each tissue was measured. Each column represents the mean ± S.E. (vertical bars) for three to six animals. *, $P < 0.05$, significantly different from each control. □, control; ■, KC500.

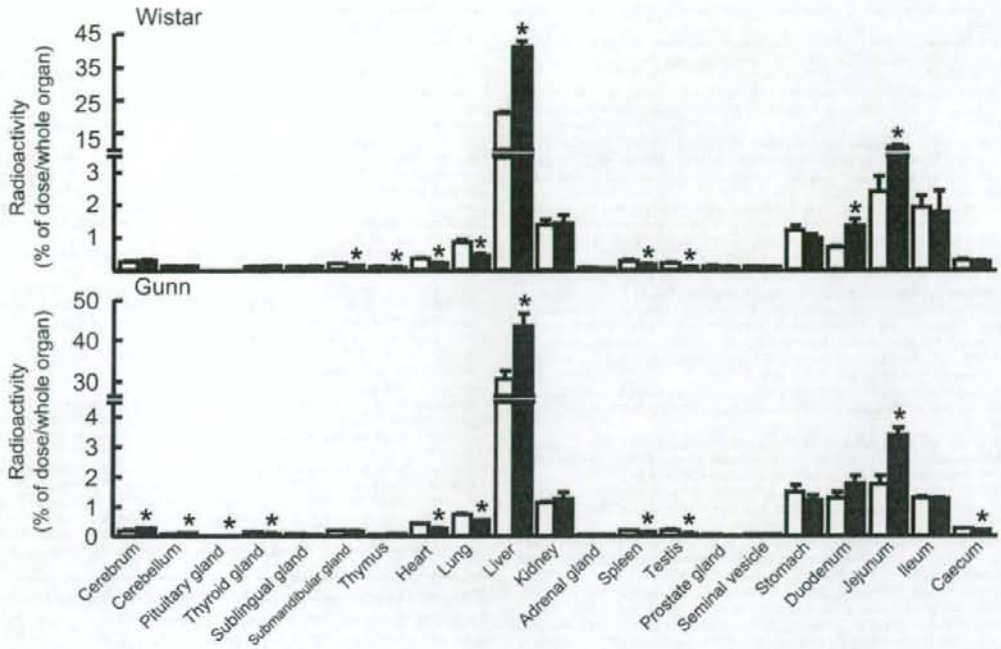

FIG. 9. Tissue distribution of [^{125}I]T_4 after administration of [^{125}I]T_4 to the KC500-pretreated Wistar and Gunn rats. The experimental conditions were the same as those described in Fig. 8. Each column represents the mean ± S.E. (vertical bars) for four to six animals. *, $P < 0.05$, significantly different from each control. □, control; ■, KC500.

TABLE 3

Liver weights after the administration of KC500 to Wistar and Gunn rats

Animals were killed at 4 days after the final administration of KC500 (10 mg/kg i.p., once daily for 10 days). The values shown are expressed as the mean ± S.E. for four to six animals.

Animal	Liver Weight	
	Control	KC500
	% of body weight	
Wistar	3.07 ± 0.04	3.81 ± 0.17*
Gunn	3.25 ± 0.08	3.38 ± 0.10

*$P < 0.01$, significantly different from each control.

TABLE 4

Accumulation of [^{125}I]T_4 in the KC500-pretreated Wistar and Gunn rat livers

The experimental conditions were the same as those described in Fig. 8. The values shown are expressed as the mean ± S.E. for four to six animals.

Animal	[^{125}I]T_4	
	Control	KC500
	% of dose/g liver	
Wistar	3.86 ± 0.18	6.01 ± 0.24*
Gunn	4.74 ± 0.43	6.33 ± 0.62

*$P < 0.001$, significantly different from each control.

T_4, because PCB and its ring-hydroxylated metabolites act as T_4 antagonists to TTR (Lans et al., 1993; Brouwer et al., 1998; Meerts et al., 2002; Kato et al., 2004). Thus, competitive inhibition by PCB and/or its metabolites would promote a decrease in the level of serum total T_4. In the present study, significant decrease in the level of [^{125}I]T_4 bound to serum TTR and increase in the level of [^{125}I]T_4 bound to serum albumin occurred in both KC500-pretreated Wistar and Gunn rats, suggesting that PCB and/or its metabolite(s) inhibit the formation of serum T_4-TTR complex.

Thus, inhibition of the T_4-TTR formation might lead to change in the tissue distribution of T_4. Therefore, to clarify this, we administered [^{125}I]T_4 to KC500-pretreated Wistar and Gunn rats and, thereafter, determined the levels of [^{125}I]T_4 in their tissues. In addition, since [^{125}I]T_4 in either plasma or tissues is known to be stable during 48 h (Oppenheimer et al., 1968), the radioactivity detected in the serum and tissues would be attributed to [^{125}I]T_4 in each tissue. Marked increases in the mean total body clearance of [^{125}I]T_4 and in the steady-state distribution volume of [^{125}I]T_4 were observed in the KC500-pretreated rats. A tissue-to-serum concentration ratio (K_p value) was greater in several tissues, especially the liver, of the KC500-pretreated Wistar and Gunn rats than in the corresponding control (KC500-untreated) rat tissues. In addition, in both KC500-pretreated Wistar and Gunn rats, more than 40% of the [^{125}I]T_4 dosed was accumulated in the liver.

In conclusion, the present findings confirmed that PCB-induced decrease in serum T_4 occurs not only in Wistar rats but also in Gunn (UGT1A-deficient) rats and further led to a hypothesis that the PCB-induced decrease occurs through increase in accumulation (transportation from serum to liver) of T_4 in the liver, rather than through induction of hepatic T_4-UDP-GT. In addition, the increased accumulation in the liver might be attributed to the PCB- and its metabolite(s)-mediated inhibition of formation of serum T_4-TTR complex.

References

Barter RA and Klaassen CD (1992a) UDP-glucuronosyltransferase inducers reduce thyroid hormone levels in rats by an extrathyroidal mechanism. *Toxicol Appl Pharmacol* **113**:36–42.
Barter RA and Klaassen CD (1992b) Rat liver microsomal UDP-glucuronosyltransferase activity

toward thyroxine: characterization, induction, and form specificity. *Toxicol Appl Pharmacol* **115**:261–267.

Barter RA and Klaassen CD (1994) Reduction of thyroid hormone levels and alteration of thyroid function by four representative UDP-glucuronosyltransferase inducers in rats. *Toxicol Appl Pharmacol* **128**:9–17.

Benathan M, Lemarchand-Beraud T, Berthier C, Gautier A, and Gardiol D (1983) Thyroid function in Gunn rats with genetically altered thyroid hormone catabolism. *Acta Endocrinol* **102**:71–79.

Brouwer A, Morse DC, Lans MC, Schuur AG, Murk AJ, Klasson-Wehler E, Bergman Å, and Visser TJ (1998) Interactions of persistent environmental organohalogens with the thyroid hormone system: mechanisms and possible consequences for animal and human health. *Toxicol Ind Health* **14**:59–84.

Burke MD, Thompson S, Elcombe CR, Halpert J, Haaparanta T, and Mayer RT (1985) Ethoxy-, pentoxy- and benzyloxyphenoxazones and homologues: a series of substrates to distinguish between different induced cytochromes P-450. *Biochem Pharmacol* **34**:3337–3345.

Craft ES, DeVito MJ, and Crofton KM (2002) Comparative responsiveness of hypothyroxinemia and hepatic enzyme induction in Long-Evans rats versus C57BL/6J mice exposed to TCDD-like and phenobarbital-like polychlorinated biphenyl congeners. *Toxicol Sci* **68**:372–380.

Davis PJ, Spaulding SW, and Gregerman RI (1970) The three thyroxine-binding proteins in rat serum: binding capacities and effects of binding inhibitors. *Endocrinology* **87**:978–986.

Hallgren S, Sinjari T, Håkansson H, and Darnerud PO (2001) Effects of polybrominated diphenyl ethers (PBDEs) and polychlorinated biphenyls (PCBs) on thyroid hormone and vitamin A levels in rats and mice. *Arch Toxicol* **75**:200–208.

Haraguchi K, Koga N, and Kato Y (2005) Comparative metabolism of polychlorinated biphenyls and tissue distribution of persistent metabolites in rats, hamsters, and guinea pigs. *Drug Metab Dispos* **33**:373–380.

Hood A, Allen ML, Liu Y, Liu J, and Klaassen CD (2003) Induction of T_4 UDP-GT activity, serum thyroid stimulating hormone, and thyroid follicular cell proliferation in mice treated with microsomal enzyme inducers. *Toxicol Appl Pharmacol* **188**:6–13.

Hood A, Hashmi R, and Klaassen CD (1999) Effects of microsomal enzyme inducers on thyroid-follicular cell proliferation, hyperplasia, and hypertrophy. *Toxicol Appl Pharmacol* **160**:163–170.

Ikushiro S, Emi Y, and Iyanagi T (1995) Identification and analysis of drug-responsive expression of UDP-glucuronosyltransferase family 1 (UGT1) isozyme in rat hepatic microsomes using anti-peptide antibodies. *Arch Biochem Biophys* **324**:267–272.

Ikushiro S, Emi Y, and Iyanagi T (1997) Protein-protein interactions between UDP-glucuronosyltransferase isozymes in rat hepatic microsomes. *Biochemistry* **36**:7154–7161.

Kato Y, Haraguchi K, Kawashima M, Yamada S, Masuda Y, and Kimura R (1995) Induction of hepatic microsomal drug-metabolizing enzymes by methylsulfonyl metabolites of polychlorinated biphenyl congeners in rats. *Chem-Biol Interact* **95**:257–268.

Kato Y, Haraguchi K, Yamazaki T, Ito Y, Miyajima S, Nemoto K, Koga N, Kimura R, and Degawa M (2003) Effects of polychlorinated biphenyls, Kanechlor-500, on serum thyroid hormone levels in rats and mice. *Toxicol Sci* **72**:235–241.

Kato Y, Ikushiro S, Haraguchi K, Yamazaki T, Ito Y, Suzuki H, Kimura R, Yamada S, Inoue T, and Degawa M (2004) A possible mechanism for decrease in serum thyroxine level by polychlorinated biphenyls in Wistar and Gunn rats. *Toxicol Sci* **81**:309–315.

Kato Y, Suzuki H, Ikushiro S, Yamada S, and Degawa M (2005) Decrease in serum thyroxine level by phenobarbital in rats is not necessarily dependent on increase in hepatic UDP-glucuronosyltransferase. *Drug Metab Dispos* **33**:1608–1612.

Lans MC, Klasson-Wehler E, Willemsen M, Meussen E, Safe S, and Brouwer A (1993) Structure-dependent, competitive interaction of hydroxy-polychlorobiphenyls, -dibenzo-*p*-dioxins and -dibenzofurans with human transthyretin. *Chem-Biol Interact* **88**:7–21.

Liu J, Liu Y, Barter RA, and Klaassen CD (1995) Alteration of thyroid homeostasis by UDP-glucuronosyltransferase inducers in rats: a dose-response study. *J Pharmacol Exp Ther* **273**:977–985.

Lowry OH, Rosebrough NJ, Farr AL, and Randall RJ (1951) Protein measurement with the Folin phenol reagent. *J Biol Chem* **193**:265–275.

Luquita MG, Catania VA, Pozzi EJS, Veggi LM, Hoffman T, Pellegrino JM, Ikushiro S, Emi Y, Iyanagi T, Vore M, and Mottino AD (2001) Molecular basis of perinatal changes in UDP-glucuronosyltransferase activity in maternal rat liver. *J Pharmacol Exp Ther* **298**:49–56.

Meerts IATM, Assink Y, Cenijn PH, van den Berg JHJ, Weijers BM, Bergman Å, Koeman JH, and Brouwer A (2002) Placental transfer of a hydroxylated polychlorinated biphenyl and effects on fetal and maternal thyroid hormone homeostasis in the rat. *Toxicol Sci* **68**:361–371.

Miyawaki I, Moriyasu M, Funabashi H, Yasuba M, and Matsuoka N (2003) Mechanism of clobazam-induced thyroidal oncogenesis in male rats. *Toxicol Lett* **145**:291–301.

Oppenheimer JH, Bernstein G, and Surks MI (1968) Increased thyroxine turnover and thyroidal function after stimulation of hepatocellular binding of thyroxine by phenobarbital. *J Clin Invest* **47**:1399–1406.

Tabata K, Yamaoka K, Kaibara A, Suzuki S, Terakawa M, and Hara T (1999) Moment analysis program available on Microsoft Excel®. *Xenobio Metab Dispos* **14**:286–293.

Van Birgelen APJM, Smit EA, Kampen IM, Groeneveld CN, Fase KM, van der Kolk J, Poiger H, van den Berg M, Koeman JH, and Brouwer A (1995) Subchronic effects of 2,3,7,8-TCDD or PCBs on thyroid hormone metabolism: use in risk assessment. *Eur J Pharmacol* **293**:77–85.

Visser TJ (1996) Pathways of thyroid hormone metabolism. *Acta Med Austriaca* **23**:10–16.

Address correspondence to: Dr. Yoshihisa Kato, Kagawa School of Pharmaceutical Sciences, Tokushima Bunri University, 1314-1, Shido, Sanuki, Kagawa 769-2193, Japan. E-mail: kato@kph.bunri-u.ac.jp

Arch Pharm Res Vol 30, No 4, 444-452, 2007

Archives of Pharmacal Research
http://apr.psk.or.kr

Gene Expression Profiles in T24 Human Bladder Carcinoma Cells by Inhibiting an L-type Amino Acid Transporter, LAT1

Shadi Baniasadi[1,2], Arthit Chairoungdua[2], Yuji Iribe[2], Yoshikatsu Kanai[2], Hitoshi Endou[2], Ken-ichi Aisaki[3], Katsuhide Igarashi[3], and Jun Kanno[3]

[1]National Research Institute of Tuberculosis and Lung Diseases, Shaheed Beheshti University of Medical Science, Tehran, Iran, [2]Department of Pharmacology and Toxicology, Kyorin University School of Medicine, 6-20-2 Shinkawa, Mitaka, Tokyo 181-8611, Japan, and [3]Division of Cellular & Molecular Toxicology, National Institute of Health Sciences, Kamiyoga 1-18-1, Setagaya-ku, Tokyo 158-8501, Japan

(Received November 13, 2006)

Inhibition of LAT1 (L-type amino acid transporter 1) activity in tumor cells could be effective in the inhibition of tumor cell growth by depriving tumor cells of essential amino acids. Because of the high level of expression of LAT1 in tumor cells, LAT1 inhibitors would be useful for anticancer therapy in suppressing tumor growth without affecting normal tissues. In recent years, cDNA microarray technique is useful technology for anticancer drug development. It allows identifying and characterizing new targets for developments in cancer drug therapy through the understanding genes involved in drug action. The present study was designed to investigate gene expression profile induced by LAT1 inhibitor using gene chip technology. Human bladder carcinoma cells (T24 cells) were treated with classical system L inhibitor 2-aminobicyclo-(2, 2, 1)-heptane-2-carboxylic acid (BCH). Gene chip experiment was applied for treated and untreated cells after 3 and 12 h. Two independent experiments with a high degree of concordance identified the altered expression of 151 and 200 genes after 3 and 12 h BCH treatment. Among these genes, 132 and 13 were up-regulated and 19 and 187 were down-regulated by 3 and 12 h BCH treatment respectively. We found that BCH affected the expression of a large number of genes that are related to the control of cell survival and physiologic behaviors. These data are useful for understanding of intracellular signaling of cell growth inhibition induced by LAT1 inhibitors as candidate for anticancer drug therapy.

Key words: BCH, Gene expression, Microarray, Bladder carcinoma cells, LAT1

INTRODUCTION

System L is a major nutrient transport system responsible for the Na^+-independent transport of large neutral amino acids including several essential amino acids (Christensen, 1990; Oxender and Christensen, 1963). In malignant tumors, a system L transporter L-type amino acid transporter 1 (LAT1) is up-regulated to support tumor cell growth (Kanai *et al.*, 1998; Sang *et al.*, 1995; Wolf *et al.*, 1996; Yanagida *et al.*, 2001) . It is proposed that the manipulation of system L activity, in particular that of LAT1, would have therapeutic implications. The inhibition of LAT1 activity in tumor cells could be effective in the inhibition of tumor cell growth by depriving tumor cells of essential amino acids (Kanai and Endou, 2001). Our previous studies have revealed that T24 cells express LAT1 in the plasma membrane together with its associating protein 4F2hc that inhibited by a system L-specific inhibitor 2-aminobicyclo-(2, 2, 1)-heptane-2-carboxylic acid (BCH) (Kim *et al.*, 2002; Yanagida *et al.*, 2001). An increased understanding of molecular mechanisms of LAT1 inhibitors will lead to the development LAT1 inhibitors for anticancer drug therapy.

cDNA microarray analysis permits the simultaneous and rapid analysis of the expression of tens of thousands of genes, and, in turn, provides an opportunity for determining the effects of anticancer agents. This technology will contribute to the more accurate development of therapeutic strategies and will help to determine the molecular mechanism(s) of action of chemopreventive and/or therapeutic agents (Li and Sarkar 2002; Macgregor and Squire,

Correspondence to: Shadi Baniasadi, National Research Institute of Tuberculosis and Lung Diseases Shaheed Beheshti University of Medical Science Tehran Iran
E-mail: sbaniasadi@yahoo.com, baniasadi@nritld.ac.ir

2002). To better understand the precise molecular mechanisms by which BCH exerts its effects on T24 bladder carcinoma cells, we utilized a cDNA microarray to interrogate the mRNA levels of 39,000 genes and to determine the gene expression profiles of T24 bladder carcinoma cells treated with BCH.

MATERIALS AND METHODS

Cell culture and growth inhibition

T24 human bladder cancer cells were cultured in the growth medium (minimum essential medium supplemented with 10% fetal bovine serum) in a 5% CO_2 atmosphere at 37°C. For growth inhibition, 60 h after seeding (during logarithmic phase) T24 cells were treated with 20 mM BCH for 3 and 12 h.

cDNA microarray analysis for gene expression profiles

T24 cells were treated with 20 mM BCH for 3 and 12 h. The rationale for choosing these time points was to capture gene expression profiles of early response genes, genes that may be involved during the onset of growth inhibition. Total RNA from each sample was isolated by Trizol (Invitrogen) and purified by RNeasy Mini Kit and RNase-free DNase Set (QIAGEN, Valencia, CA) according to the manufactures' protocols. cDNA for each sample was synthesized by using Superscript cDNA Synthesis Kit (Invitrogen) using T7-(dT)24 primer instead of the oligo (dT) provided in the kit. The biotin-labeled cRNA was transcripted in vitro from cDNA using a BioArray HighYield RNA Transcript Labeling Kit (ENZO Biochem, New York, NY) and purified using an RNeasy Mini Kit. The purified cRNA was fragmented by incubation in fragmentation buffer (200 mmol/L Tris-acetate pH 8.1, 500 mmol/L KOAc, 150 mmol/L MgOAc) at 95°C for 35 min and chilled on ice. The fragmented labeled cRNA was applied to Human Genome U133 Array (Affymetrix, Santa Clara, CA), which contains 39,000 human gene cDNA probes, and hybridized to the probes in the array. After washing and staining, the arrays were scanned using a HP GeneArray Scanner (Hewlett-Packard, Palo Alto, CA). Two independent experiments were performed to verify the reproducibility of results.

Microarray data normalization and analysis

Data analysis was performed with the GeneChip Expression Analysis software (Affymetrix) and GeneSpring TM software (Silicon Genetics, Redwood, CA, U.S.A.). The differences in hybridization efficiency among arrays were equalized by intensities of spiked-in control mRNAs added to the sample in proportion to its DNA content (Kanno *et al.*, 2006). In a set of GeneChip experiments comparing the same sample hybridized to two different arrays, method-associated experimental artifacts produced less than two-fold differences between two identical samples. Thus, genes displayed over two-fold expression change were subjected to further testing. GeneChip array HG-U133A represents 22283 transcripts and the genes whose absolute call judged "present" in at least 1 sample were used for further analysis.

RESULTS

Cell growth inhibition by BCH treatment

Cell count showed that the treatment of T24 bladder cancer cells with BCH, time dependently inhibited cell proliferation (Fig. 1), demonstrating the growth inhibitory effect of BCH. These results are consistent with our previous study. This inhibition of cell proliferation could be due to altered regulation of gene expression by BCH.

Regulation of gene expression by BCH treatment

The gene expression profiles of T24 cells treated with BCH were assessed using cDNA microarray. Two inde-

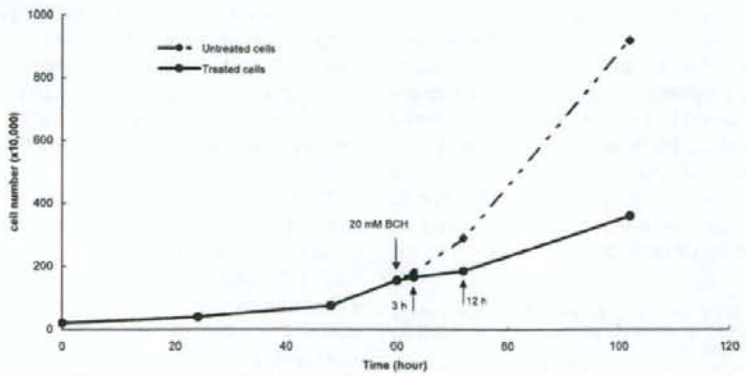

Fig. 1. T24 cell growth curve. BCH was added to treated cells 60 h after seeding.

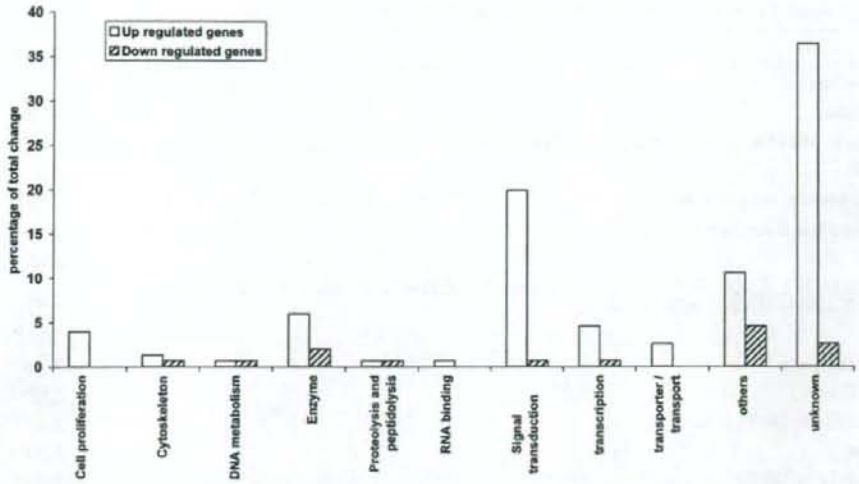

Fig. 2. Effect of BCH on gene expression after 3 h. Expression of many genes altered in T24 cells treated with BCH for 3 h.

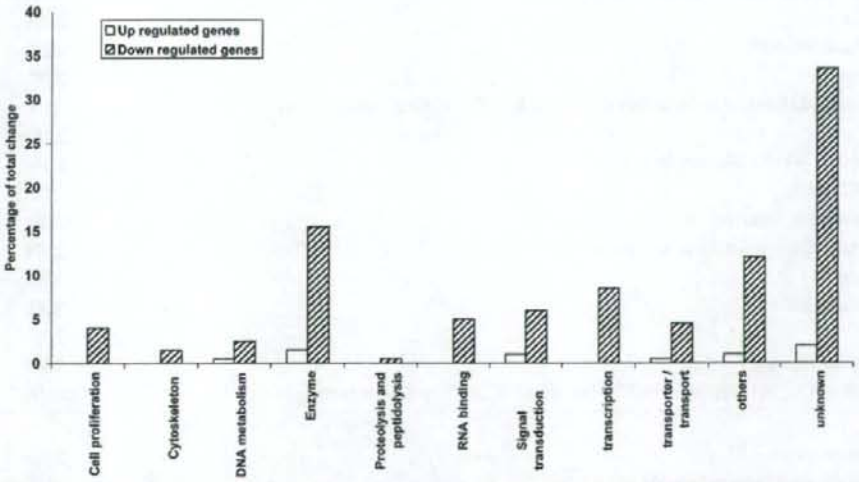

Fig 3. Effect of BCH on gene expression after 12 h. Expression of many genes altered in T24 cells treated with BCH for 12 h.

pendent experiments showed the altered expression of 151 and 200 genes at the mRNA level after 3 and 12 h BCH treatment. Among these genes, 132 and 13 were up-regulated and 19 and 187 were down-regulated by 3 and 12 h BCH treatment respectively. Expression of genes altered as early as 3 and 12 h of BCH treatment and was significantly up-regulated after 3 h and down-regulated after 12 h (Figs. 2 and 3). We found that after 3 h, BCH up-regulated genes that are involved mainly in signal transduction, enzyme reaction, transcription, cell proliferation and transport (Table I). On the other hand after 12 h, BCH down-regulated genes that are related mainly to enzyme reaction, transcription, signal transduction, RNA binding, transport, cell proliferation and DNA metabolism (Table II).

DISCUSSION

For continuous growth and proliferation, rapidly dividing tumor cells require more supply of sugars and amino acids. They are supported by the up regulation of transporters specialized for those nutrients. Transporters for essential amino acids are particularly important since they

Table I. Fold changes of specific genes in T24 cells treated with BCH for 3 h

genes	foldchange	t-test p-value
signal transduction		
Hypothetical protein	3.100	0.156
th79e05.x1 Soares_NhHMPu_S1 Homo sapiens cDNA clone IMAGE:2124896 3', mRNA sequence.	2.871	0.045
Sorting nexin 11	2.691	0.012
GABA(A) receptor-associated protein like 1	2.674	0.083
Down syndrome critical region gene 1	2.666	0.058
Interleukin 8	2.629	0.123
wd41c03.x1 Soares_NFL_T_GBC_S1 Homo sapiens cDNA clone IMAGE:2330692 3' similar to TR:O00538 O00538 F25B3.3 KINASE LIKE PROTEIN. ;, mRNA sequence.	2.596	0.439
Interleukin 8	2.534	0.087
IL2-inducible T-cell kinase	2.526	0.371
Protein kinase C, beta 1	2.427	0.151
Insulin-like growth factor binding protein 3	2.377	0.130
Vav 3 oncogene	2.267	0.053
Fibroblast growth factor 12B	2.237	0.127
CD53 antigen	2.216	0.106
MAD (mothers against decapentaplegic, Drosophila) homolog 7	2.194	0.073
GRO2 oncogene	2.186	0.020
G protein-coupled receptor 27	2.178	0.308
Adhesion glycoprotein	2.173	0.061
qq08e12.x1 Soares_NhHMPu_S1 Homo sapiens cDNA clone IMAGE:1931950 3', mRNA sequence.	2.159	0.027
Epiregulin	2.152	0.021
Gamma-aminobutyric acid (GABA) receptor, rho 2	2.143	0.159
DKFZP564L0862 protein	2.125	0.505
Insulin-like growth factor binding protein 1	2.080	0.216
GTP-binding protein overexpressed in skeletal muscle	2.074	0.056
Syntrophin, gamma 1	2.053	0.388
Adenosine A1 receptor	2.046	0.024
Inhibin, alpha	2.020	0.003
Frizzled (Drosophila) homolog 7	2.008	0.055
601763146F1 NIH_MGC_20 Homo sapiens cDNA clone IMAGE:4026010 5', mRNA sequence.	2.008	0.101
enzyme		
Cytosolic beta-glucosidase	2.668	0.209
UDP glycosyltransferase 1 family, polypeptide A1	2.355	0.014
wg36d09.x1 Soares_NSF_F8_9W_OT_PA_P_S1 Homo sapiens cDNA clone IMAGE:2367185 3', mRNA sequence.	2.287	0.072
Arginase, liver	2.201	0.339
Peptidylprolyl isomerase A (cyclophilin A)	2.166	0.423
ov13a06.x1 NCI_CGAP_Kid3 Homo sapiens cDNA clone IMAGE:1637170 3' similar to WP:R07B7.5 CE06267 ;, mRNA sequence.	2.116	0.270
cytochrome P450IIE1; Human cytochrome P450IIE1 (ethanol-inducible) gene, complete cds.	2.075	0.279
Keratin, hair, basic, 6 (monilethrix)	2.072	0.043
Protein kinase, Y-linked	2.028	0.430
transcription		
Homeo box A6	2.294	0.062
yf31g02.s1 Soares fetal liver spleen 1NFLS Homo sapiens cDNA clone IMAGE:128498 3', mRNA sequence.	2.024	0.259
Runt-related transcription factor 2	2.009	0.048

Table I. Continued

genes	foldchange	t-test p-value
transcription		
Cardiac-specific homeo box	2.095	0.170
wa17f11.x1 NCI_CGAP_Kid11 Homo sapiens cDNA clone IMAGE:2298381 3' similar to TR:Q15886 Q15886 X-LINKED NUCLEAR PROTEIN ;, mRNA sequence.	2.435	0.276
Cofactor required for Sp1 transcriptional activation, subunit 3 (130kD)	2.376	0.132
Wolf-Hirschhorn syndrome candidate 1-like 1	2.047	0.013
cell proliferation		
Tumor necrosis factor receptor superfamily, member 9	2.651	0.084
Interleukin 1, beta	2.233	0.001
Interleukin 1, alpha	2.150	0.019
Interleukin 12A (natural killer cell stimulatory factor 1, cytotoxic lymphocyte maturation factor 1, p35)	2.124	0.162
Epidermal growth factor receptor (avian erythroblastic leukemia viral (v-erb-b) oncogene homolog)	2.093	0.066
nad20g10.x1 NCI_CGAP_Lu24 Homo sapiens cDNA clone IMAGE:3366330 3', mRNA sequence.	2.031	0.087
transport		
Solute carrier family 4, sodium bicarbonate cotransporter-like, member 10	3.528	0.166
UI-H-BW0-ajo-f-12-0-UI.s1 NCI_CGAP_Sub6 Homo sapiens cDNA clone IMAGE:2732686 3', mRNA sequence.	2.468	0.423
Solute carrier family 35 (UDP-N-acetylglucosamine (UDP-GlcNAc) transporter), member 3	2.110	0.152
Solute carrier family 21 (organic anion transporter), member 3	2.031	0.030

Table II. Fold changes of specific genes in T24 cells treated with BCH for 12 h

gene	foldchange	t-test p-value
enzyme		
GDP-mannose pyrophosphorylase B	0.306	0.078
AU121975 MAMMA1 Homo sapiens cDNA clone MAMMA1001393 5', mRNA sequence.	0.319	0.235
Polymerase (DNA directed), mu	0.334	0.159
Adenylate kinase 2	0.353	0.015
F-box only protein 9	0.362	0.057
Stearoyl-CoA desaturase (delta-9-desaturase)	0.362	0.046
N-myristoyltransferase 1	0.370	0.095
Protein phosphatase 2 (formerly 2A), regulatory subunit B" (PR 72), alpha isoform and (PR 130), beta isoform	0.383	0.078
Homo sapiens Scd mRNA for stearoyl-CoA desaturase, complete cds.	0.384	0.009
qd05f07.x1 Soares_placenta_8to9weeks_2NbHP8to9W Homo sapiens cDNA clone IMAGE:1722853 3' similar to SW:ER19_HUMAN P53602 DIPHOSPHOMEVALONATE DECARBOXYLASE ;contains MER22.b1 MSR1 repetitive element ;, mRNA sequence.	0.404	0.013
602022620F1 NCI_CGAP_Brn67 Homo sapiens cDNA clone IMAGE:4158005 5', mRNA sequence.	0.406	0.020
N-acetylglucosaminidase, alpha- (Sanfilippo disease IIIB)	0.407	0.279
3-hydroxybutyrate dehydrogenase (heart, mitochondrial)	0.409	0.238
Creatine kinase, mitochondrial 2 (sarcomeric)	0.440	0.135
Phosphodiesterase 4D, cAMP-specific (dunce (Drosophila)-homolog phosphodiesterase E3)	0.441	0.020
qi08f09.x1 Soares_NhHMPu_S1 Homo sapiens cDNA clone IMAGE:1855913 3', mRNA sequence.	0.454	0.071
AL525798 LTI_NFL003_NBC3 Homo sapiens cDNA clone CS0DC013YB08 5 prime, mRNA sequence.	0.454	0.020
KIAA0015 gene product	0.455	0.043
Glutaryl-Coenzyme A dehydrogenase	0.467	0.082
Polynucleotide kinase 3'-phosphatase	0.470	0.079
Enolase 2, (gamma, neuronal)	0.471	0.008
xn86c10.x1 Soares_NFL_T_GBC_S1 Homo sapiens cDNA clone IMAGE:2701362 3' similar to TR:Q99766 Q99766 HYPOTHETICAL 15.7 KD PROTEIN. ; mRNA sequence.	0.481	0.112

Table II. Continued

gene	foldchange	t-test p-value
enzyme		
Serine hydroxymethyltransferase 1 (soluble)	0.483	0.092
Crystallin, zeta (quinone reductase)-like 1	0.486	0.042
xd94e03.x1 Soares_NFL_T_GBC_S1 Homo sapiens cDNA clone IMAGE:2605276 3' similar to WP:Y116A8C.27 CE23335 ;, mRNA sequence.	0.488	0.213
Aminoacylase 1	0.488	0.016
H.sapiens pseudogene for mitochondrial ATP synthase c subunit (P2 form).	0.491	0.088
zi27a06.s1 Soares_fetal_liver_spleen_1NFLS_S1 Homo sapiens cDNA clone IMAGE:431986 3', mRNA sequence.	0.491	0.061
Fatty-acid-Coenzyme A ligase, long-chain 3	0.492	0.069
Triosephosphate isomerase 1	0.494	0.322
Tumor necrosis factor receptor superfamily, member 6b, decoy	0.495	0.000
transcription		
Paired box gene 3 (Waardenburg syndrome 1)	0.342	0.260
Paired box gene 8	0.423	0.218
AU118165 HEMBA1 Homo sapiens cDNA clone HEMBA1003008 5', mRNA sequence.	0.466	0.057
Core promoter element binding protein	0.447	0.016
Death effector domain-containing	0.484	0.028
Trinucleotide repeat containing 11 (THR-associated protein, 230 kDa subunit)	0.498	0.002
NS1-binding protein	0.335	0.018
Hypothetical protein	0.484	0.031
602437464F1 NIH_MGC_46 Homo sapiens cDNA clone IMAGE:4555622 5', mRNA sequence.	0.486	0.027
601872674F1 NIH_MGC_54 Homo sapiens cDNA clone IMAGE:4096483 5', mRNA sequence.	0.432	0.002
Cofactor required for Sp1 transcriptional activation, subunit 9 (33kD)	0.472	0.157
Zinc finger protein 254	0.489	0.374
Ring finger protein 1	0.404	0.154
Nuclear respiratory factor 1	0.376	0.111
HSPC028 protein	0.486	0.009
KIAA0664 protein	0.496	0.031
signal transduction		
Regulator of G-protein signalling 4	0.109	0.029
Integrin, alpha 9	0.164	0.015
CAMP responsive element modulator	0.255	0.158
Endothelin receptor type B	0.302	0.011
AL514445 LTI_NFL006_PL2 Homo sapiens cDNA clone CL0BB010ZF08 3 prime, mRNA sequence.	0.322	0.008
Ankyrin 1, erythrocytic	0.340	0.094
wu94e06.x1 NCI_CGAP_Kid3 Homo sapiens cDNA clone IMAGE:2527714 3' similar to gb:U07358 MIXED LINEAGE KINASE 2 (HUMAN);, mRNA sequence.	0.342	0.098
ADP-ribosylation factor related protein 1	0.345	0.030
Melanoma cell adhesion molecule	0.351	0.053
7o43e03.x1 NCI_CGAP_Kid11 Homo sapiens cDNA clone IMAGE:3577036 3', mRNA sequence.	0.431	0.095
LIM domain only 7	0.439	0.045
Enigma (LIM domain protein)	0.492	0.036
RNA binding		
qb33c06.x1 Soares_pregnant_uterus_NbHPU Homo sapiens cDNA clone IMAGE:1698058 3', mRNA sequence.	0.215	0.055
RNA binding motif protein 12	0.386	0.007

Table II. Continued

gene	foldchange	t-test p-value
RNA binding		
Polyadenylate binding protein-interacting protein 1	0.411	0.029
Splicing factor, arginine/serine-rich 6	0.419	0.003
AU146237 HEMBA1 Homo sapiens cDNA clone HEMBA1007233 3', mRNA sequence.	0.422	0.013
Polyadenylate binding protein-interacting protein 1	0.458	0.058
Splicing factor, arginine/serine-rich 7 (35kD)	0.472	0.060
DEAD-box protein abstrakt	0.493	0.035
Mitochondrial ribosomal protein L12	0.495	0.138
Heterogeneous nuclear ribonucleoprotein D-like	0.497	0.025
transport		
wc46f12.x1 NCI_CGAP_Pr28 Homo sapiens cDNA clone IMAGE:2321711 3' similar to TR:O14564 O14564 HYPOTHETICAL 67.1 KD PROTEIN. ;, mRNA sequence.	0.338	0.072
Uncoupling protein 2 (mitochondrial, proton carrier)	0.385	0.020
Adaptor-related protein complex 3, sigma 2 subunit	0.278	0.110
Solute carrier family 4, anion exchanger, member 2 (erythrocyte membrane protein band 3-like 1)	0.408	0.134
Hypothetical protein FLJ14038	0.469	0.002
Solute carrier family 4, sodium bicarbonate cotransporter-like, member 10	0.395	0.124
N amino acid transporter 3	0.451	0.072
Solute carrier family 25 (mitochondrial carrier; oxoglutarate carrier), member 11	0.467	0.017
Solute carrier family 19 (folate transporter), member 1	0.490	0.068
cell proliferation		
Deoxyhypusine synthase	0.175	0.026
Deoxyhypusine synthase	0.372	0.039
ba69f11.x1 NIH_MGC_20 Homo sapiens cDNA clone IMAGE:2905677 3' similar to SW:CL6_RAT Q08755 INSULIN-INDUCED GROWTH RESPONSE PROTEIN CL-6 ;, mRNA sequence.	0.437	0.008
Cyclin H	0.455	0.043
Bridging integrator 1	0.487	0.071
V-Ki-ras2 Kirsten rat sarcoma 2 viral oncogene homolog	0.489	0.171
Deoxyhypusine synthase	0.494	0.031
U69567 Soares infant brain 1NIB Homo sapiens cDNA clone c-2mell, mRNA sequence.	0.499	0.072
DNA metabolism		
BRCA1-interacting protein 1; BRCA1-associated C-terminal helicase 1	0.410	0.028
Uracil-DNA glycosylase	0.434	0.102
Nth (E.coli endonuclease III)-like 1	0.443	0.017
DNA (cytosine-5-)-methyltransferase 2	0.469	0.209
602504673F1 NIH_MGC_77 Homo sapiens cDNA clone IMAGE:4617907 5', mRNA sequence.	0.470	0.200

are indispensable for protein synthesis (Christensen, 1990; McGivan and Pastor-Anglada, 1994). Among the amino acid transport systems described, system L is a major rout for providing cells with large neutral amino acids including branched or aromatic amino acids (Comford *et al.*, 1992; Gomes and Soares-da-Silva, 1999). LAT1 is a system L amino acid transporter which transports a lot of essential amino acids. It is proposed to be at least one of the amino acids transporters essential for tumor cell growth (Yanagida *et al.*, 2001). High level of expression of LAT1 in tumor cells was indicated in tumor masses of various tissue origins as well as various tumor cell lines to support the high protein synthesis for cell growth and cell activation (Kanai *et al.*, 1998; Sang *et al.*, 1995; Wolf *et al.*, 1996). Since LAT1 is an amino acid transporter essential for tumor cell growth, one can expect that inhibition of LAT1 function may be a rational to anti-cancer therapy to suppress tumor growth (Kim *et al.*, 2004). BCH

is an amino acid-related compound which has been used as a selective inhibitor of system L (Christensen, 1990; Christensen *et al.*, 1969). Our previous studies have shown that BCH exert inhibitory effects on T24 cells through inhibition of LAT1 (Kim *et al.*, 2002). We confirmed this for T24 cells by showing that BCH in logarithmic phase of cell growth curve inhibits cell proliferation (Fig. 1).

Determining of gene expression profiles of T24 bladder carcinoma cells after BCH treatment is important for designing new anticancer drugs. It is possible to analyze the expression profiles of a large number of genes simultaneously using microarray. In this study, we utilized the high throughput gene chip, which contains 39,000 known genes, to determine the alternation of gene expression profiles of T24 bladder carcinoma cells exposed to BCH. Our results from cDNA microarray provided a complex cellular and molecular response to BCH treatment that likely to be mediated by a variety of regulatory pathways. We found that the molecular response to BCH in T24 bladder carcinoma cells involved inhibition or induction of genes that are related to biochemical, biological and regulatory processes in the cells. These genes have specific functions in cell proliferation, DNA metabolism, enzyme reaction, RNA binding, signal transduction, transcription, and transport. General tendency was up-regulation of these genes at 3 h and down-regulation at 12 h after BCH treatment (Fig. 2 and 3). These results suggest that inhibition of LAT1 by BCH may modulate the expression of first-response genes at an earlier stage (3 h), and in turn, alter the expression of intracellular second messenger molecules, resulting in cell adaptation for survival. At later stage (12 h), cellular response to BCH may involve modulation of gene expression for cell growth inhibition. For example up regulation of genes that are involved in cell proliferation at 3 h provide cellular pathways for survival and adaptation whereas down regulation of this group of genes at 12 h inhibit cell growth. Expression of interleukin 1 that stimulates proliferation (Beales, 2002; Kaden *et al.*, 2003; Olman *et al.*, 2002), significantly increased after 3 h and expression of deoxyhypusine synthase that causes growth in mammalian cells (Chen *et al.*, 1996; Park *et al.*, 1994; Shi *et al.*, 1996) decreased after 12 h, suggesting that BCH may inhibit cell growth through regulation of the expression of these important genes related to cell proliferation.

In signal transduction group, up regulation of Sorting nexin 11, GRO2 oncogene, Epiregulin, Adenosine A1 receptor, Inhibin alpha and down regulation of KIAA1075 protein were observed at 3 h whereas down regulation of Regulator of G-protein signalling 4, Integrin alpha 9, Endothelin receptor type B, ADP-ribosylation factor related protein 1, LIM domain only 7, Enigma (LIM domain protein) and up regulation of Hypothetical protein and Opsin 3 (encephalopsin, panopsin) were observed at 12 h, suggesting that cell signal transduction pathways is important for cell growth inhibition *via* LAT1 inhibitor.

In summary, we have analyzed the gene expression profiles of T24 bladder carcinoma cells exposed to BCH. BCH altered the expressions of many genes that are related to the control of cell proliferation, DNA metabolism, enzyme reaction, RNA binding, signal transduction, transcription, and transport. The gene expression profiles revealed novel molecular mechanisms by which BCH exerts its inhibitory effects on bladder carcinoma. BCH-induced regulation of these genes may be exploited for mechanism-based therapeutic strategies and new drugs development for bladder carcinoma. However, further in-depth studies are required to investigate the effects of BCH on the regulation of important cellular molecules at the protein levels to examine the effects of BCH on cellular pathways.

REFERENCES

Beales, I. L., Effect of Interlukin-1â on proliferation of gastric epithelial cells in culture. *BMC Gastroenterol.*, 2, 7 (2002).

Chen, Z. P., Yan, Y. P., Ding, Q. J., Knapp, S., Potenza, J. A., Schugar, H. J., and Chen, K. Y., Effects of inhibitors of deoxyhypusine synthase on the differentiation of mouse neuroblastoma and erythroleukemia cells. *Cancer lett.*, 105, 233-239 (1996).

Christensen, H. N., Role of amino acid transport and countertransport in nutrition and metabolism. *Physiol. Rev.*, 70, 43-77 (1990).

Christensen, H. N., Handlogten, M. E., Lam, I., Tager, H. S., and Zand, R., A bicyclic amino acid to improve discriminations among transport systems. *J. Biol. Chem.*, 244, 1510–1520 (1969).

Cornford, E. M., Young, D., Paxton, J. W., Finlay, G. J., Wilson, W. R., and Pardridge, W. M., Melphalan penetration of the blood-brain barrier via the neutral amino acid transporter in tumor-bearing brain. *Cancer Res.*, 52, 138-143 (1992).

Gomes, P. and Soares-da-Silva, P., L-DOPA transport properties in an immortalised cell line of rat capillary cerebral endothelial cells, RBE 4. *Brain Res.*, 829, 143-150 (1999).

Kaden, J. J., Dempfle, C. E., Grobholz, R., Tran, H. T., Kilic, R., Sarikoc, A., Brueckmann, M., Vahl, C., Hagl, S., Haase, K. K., and Borggrefe, M., Interleukin-1 beta promotes matrix metalloproteinase expression and cell proliferation in calcific aortic valve stenosis. *Atherosclerosis*, 170, 205-211 (2003).

Kanai, Y. and Endou, H., Heterodimeric amino acid transporters: molecular biology and pathological and pharmacological relevance. *Curr. Drug Metab.*, 2, 339-354 (2001).

Kanai, Y., Segawa, H., Miyamoto, K., Uchino, H., Takeda, E., and Endou, H., Expression cloning and characterization of a transporter for large neutral amino acids activated by the

heavy chain of 4F2 antigen (CD98). *J. Biol. Chem.*, 273, 23629–23632 (1998).

Kanno, J., Aisaki, K. I., Igarashi, K., Nakatsu, N., Ono, A., Kodama, Y., and Nagao, T., "Per cell" normalization method for mRNA measurement by quantitative PCR and microarrays. *BMC Genomics*, 7, 64 (2006).

Kim, D. K., Kanai, Y., Choi, H. W., Tangtrongsup, S., Chairoungdua, A., Babu, E., Tachampa, K., Anzai, N., Iribe, Y., and Endou, H., Characterization of the system L amino acid transporter in T24 human bladder carcinoma cells. *Biochim. Biophys. Acta*, 1565, 112-121 (2002).

Kim, D. K., Kim, I. J., Hwang, S., Kook, J. H., Lee, M. C., Shin, B. A., Bae, C. S., Yoon, J. H., Ahn, S. G., Kim, S. A., Kanai, Y., Endou, H., and Kim, J. K., System L-amino acid transporters are differently expressed in rat astrocyte and C6 glioma cells. *Neurosci. Res.*, 50, 437-446 (2004).

Li, Y. and Sarkar, F. H., Gene expression profiles of genistein-treated PC3 prostate cancer cells. *J. Nutr.*, 132, 3623-3631 (2002).

Macgregor, P. F. and Squire, J. A., Application of microarrays to the analysis of gene expression in cancer. *Clin. Chem.*, 48, 1170-1177 (2002).

McGivan, J. D. and Pastor-Anglada, M., Regulatory and molecular aspects of mammalian amino acid transport. *Biochem. J.*, 299, 321-334 (1994).

Olman, M. A., White, K. E., Ware, L. B., Cross, M. T., Zhu, S., and Matthay, M. A., Microarray analysis indicates that pulmonary edema fluid from patients with acute lung injury mediates inflammation, mitogen gene expression, and fibroblast proliferation through bioactive interleukin-1. *Chest*, 121 Suppl 3, 69-70 (2002).

Oxender, D. L. and Christensen, H. N., Evidence for two types of mediation of neutral amino acid transport in Ehrlich cells. *Nature*, 197, 765-767 (1963).

Park, M. H., Wolff, E. C., Lee, Y. B., and Folk, J. E., Antiproliferative effects of inhibitors of deoxyhypusine synthase. Inhibition of growth of Chinese hamster ovary cells by guanyl diamines. *J. Biol. Chem.*, 269, 27827-27832 (1994).

Sang, J., Lim, Y. P., Panzia, M., Finch, P., and Thompson, N. L., TA1, a highly conserved oncofetal complementary DNA from rat hepatoma, encodes an integral membrane protein associated with liver development, carcinogenesis, and cell activation. *Cancer Res.*, 55, 1152-1159 (1995).

Shi, X. P., Yin, K. C., Ahern, J., Davis, L. J., Stern, A. M., and Waxman, L., Effects of N1-guanyl-1, 7-diaminoheptane, an inhibitor of deoxyhypusine synthase, on the growth of tumorigenic cell lines in culture. *Biochim. Biophys. Acta*, 1310, 119-126 (1996).

Wolf, D. A., Wang, S., Panzia, M. A., Bassily, N. H., and Thompson, N. L., Expression of a highly conserved oncofetal gene, TA1/E16, in human colon carcinoma and other primary cancers: homology to Schistosoma mansoni amino acid permease and Caenorhabditis elegans gene products. *Cancer Res.*, 56, 5012-5022 (1996).

Yanagida, O., Kanai, Y., Chairoungdua, A., Kim, D. K., Segawa, H., Nii, T., Cha, S. H., Matsuo, H., Fukushima, J., Fukasawa, Y., Tani, Y., Taketani, Y., Uchino, H., Kim, J. Y., Inatomi, J., Okayasu, I., Miyamoto, K., Takeda, E., Goya, T., and Endou, H., Human L-type amino acid transporter 1 (LAT1): characterization of function and expression in tumor cell lines. *Biochim. Biophys. Acta*, 1514, 291-302 (2001).

0026-895X/07/7205-1171–1180$20.00
MOLECULAR PHARMACOLOGY
Copyright © 2007 The American Society for Pharmacology and Experimental Therapeutics
Mol Pharmacol 72:1171–1180, 2007

Vol. 72, No. 5
38836/3268509
Printed in U.S.A.

Evaluation of Action Mechanisms of Toxic Chemicals Using JFCR39, a Panel of Human Cancer Cell Lines[S]

Noriyuki Nakatsu, Tomoki Nakamura, Kanami Yamazaki, Soutaro Sadahiro, Hiroyasu Makuuchi, Jun Kanno, and Takao Yamori

Division of Molecular Pharmacology, Cancer Chemotherapy Center, Japanese Foundation for Cancer Research, Koto-ku, Tokyo, Japan (N.N., T.N., K.Y., T.Y.); Division of Cellular and Molecular Toxicology, Biological Safety Research Center, National Institute of Health Sciences, Setagaya-ku, Tokyo, Japan (N.N., J.K.); and Second Department of Surgery, Tokai University School of Medicine, Boseidai, Isehara-City, Kanagawa, Japan (T.N., S.S., H.M.)

Received June 6, 2007; accepted August 16, 2007

ABSTRACT

We previously established a panel of human cancer cell lines, JFCR39, coupled to an anticancer drug activity database; this panel is comparable with the NCI60 panel developed by the National Cancer Institute. The JFCR39 system can be used to predict the molecular targets or evaluate the action mechanisms of the test compounds by comparing their cell growth inhibition profiles (i.e., fingerprints) with those of the standard anticancer drugs using the COMPARE program. In this study, we used this drug activity database-coupled JFCR39 system to evaluate the action mechanisms of various chemical compounds, including toxic chemicals, agricultural chemicals, drugs, and synthetic intermediates. Fingerprints of 130 chemicals were determined and stored in the database. Sixty-nine of 130 chemicals (~60%) satisfied our criteria for the further analysis and were classified by cluster analysis of the fingerprints of these chemicals and several standard anticancer drugs into the following three clusters: 1) anticancer drugs, 2) chemicals that shared similar action mechanisms (for example, ouabain and digoxin), and 3) chemicals whose action mechanisms were unknown. These results suggested that chemicals belonging to a cluster (i.e., a cluster of toxic chemicals, a cluster of anticancer drugs, etc.) shared similar action mechanism. In summary, the JFCR39 system can classify chemicals based on their fingerprints, even when their action mechanisms are unknown, and it is highly probable that the chemicals within a cluster share common action mechanisms.

Determining the action mechanism or identifying the molecular target of a chemical with pharmacological activity or adverse side effects is highly desirable. Although various test methods are currently available for determining the action mechanisms of chemicals, such as methods based on animal models, methods based on cellular models, bacterial mutagenicity test, the uterotropic assay (Kanno et al., 2002), Hershberger test (Hershberger et al., 1953), and the reporter assay for the nuclear receptor agonists, determination of the action mechanisms of pharmacologically active chemicals, including the toxic chemicals, is still a difficult and challenging task. Therefore, it is highly desirable to develop efficient test methods for evaluating toxicity of chemicals.

A number of screening methods are currently available for discovering new anticancer drugs. One very powerful and unique approach using multiple cancer cell lines was developed at NCI (Paull et al., 1989; Weinstein et al., 1992, 1997) and in our laboratory (Yamori et al., 1999; Dan et al., 2002, 2003; Yamori, 2003; Nakatsu et al., 2005; Akashi and Yamori, 2007; Akashi et al., 2007; Nakamura et al., 2007). This bioinformatics-based approach enables mechanism-oriented evaluation of anticancer drugs. For example, we can evaluate the cell toxicity in vitro by determining the 50% growth inhibition (GI50), total growth inhibition, and 50% lethal concentration across a panel of 39 human cancer cell lines (JFCR39). We can also predict the molecular targets or evaluate the action mechanisms of the test compounds by comparing the cell growth inhibition profiles (termed "fingerprints") across the panel for these compounds with those of

This work was supported in part by Grant-in-Aid 17390032 for Scientific Research (B) from Japan Society for the Promotion of Science (to T.Y.); Ministry of Health, Labor, and Welfare Grants-in-Aid H15-kagaku-002, H16-kagaku-003 (to T.Y. and J.K.); Grant-in-Aid 18015049 of the Priority Area "Cancer" from the Ministry of Education, Culture, Sports, Science and Technology of Japan (to T.Y.); and grant 05-13 from National Institute of Biomedical Innovation Japan (to T.Y.)

N. N. and T. N. equally contributed to this study.

Article, publication date, and citation information can be found at http://molpharm.aspetjournals.org.

doi:10.1124/mol.107.038836.

[S] The online version of this article (available at http://molpharm.aspetjournals.org) contains supplemental material.

ABBREVIATIONS: GI50, 50% growth inhibition concentration; GI50, 50% growth inhibition; SN-38, 7-ethyl-10-hydroxycamptothecin; SV-NN, snake venom from *N. nigricollis*; SV-NNK; snake venom from *N. naja kaouthia*.

TABLE 1
List of chemicals tested. Chemical names, abbreviations, and applications/targets/mechanisms of the test compounds are summarized.

JCI No	Name	Abbreviation	Application/Target/Mechanism
−691	Trioctyltin	TOT	Organotin
−690	Triphenyltin	TPT	Organotin
−689	Dibutyltin		Organotin
−688	AM-580		RARα
−687	TTNPB		RAR
−686	13-*cis* Retinoic acid	13-*cis*	RAR
−607	Methoprene		Agricultural chemical
−606	Methoprene acid		RXR
−605	5-aza-2′-deoxycytidine	5-AzaC	Methylation
−604	Carbaryl		Agricultural chemical
−603	Acephate		Agricultural chemical
−602	Sodium arsenite		Agricultural chemical
−601	Testosterone propionate	TP	Testosterone
−600	Ethynyl estradiol	EE	Estrogenic
−599	Thiram		Agricultural chemical
−598	Dimethylformamide	DMF	Solvent
−568	α-Bungarotoxin	αBuTX	Neurotoxin
−567	Snake venom from *Trimeresurus flavoviridis*	SV-TF	Snake venom
−566	Snake venom from *Crotalus atrox*	SV-CA	Snake venom
−565	Snake venom from *Agkistrodon halys blomhoffii*	SV-AHB	Snake venom
−564	Dexamethasone	DEX	Steroid
−563	3-Methylcholanthrene	3-MC	Teratogenicity/carcinogenicity
−562	*N*-Ethyl-*N*-nitrosourea	ENU	Teratogenicity/carcinogenicity
−561	Diethylnitrosamine	DEN	Teratogenicity/carcinogenicity
−560	All *trans*-retinoic acid	ATRA	RAR + RXR
−559	9-cis Retinoic acid	9-cis	RAR
−558	Levothyroxine	T4	Thyroid hormone
−557	3-Amino-1*H*-1,2,4-triazole	3AST	Agricultural chemical
−555	2-Vinylpyridine	2VP	Synthetic intermediate
−553	Phenobarbital	PB	Antiepileptic
−552	Acetaminophen	APAP	Analgetic
−551	Isoniazid		Phthisic
−549	4-Ethylnitrobenzene	4ENB	Synthetic intermediate
−548	1,2-Dichloro-3-nitrobenzene	1,2DC3NB	Pigment/synthetic intermediate
−546	*N*-Methylaniline	NMA	Synthetic intermediate
−545	2-Aminomethylpyridine	2AMP	Synthetic intermediate
−544	1*H*-1,2,4-Triazole		Synthetic intermediate
−543	1*H*-1,2,3-Triazole		Synthetic intermediate
−542	4-Amino-2,6-dichlorophenol	4A2,6DCP	Synthetic intermediate
−541	2,4-Dinitrophenol	2,4 DNP	Agricultural chemical
−513	Capsaicin		Food constituent
−485	2-Methoxyestradiol		Estrogenic
−466	Colcemid		Spindle inhibitor
−465	2,4-Dinitrochlorobenzene	2,4DCB	Pigment/mutagenesis
−464	Troglitazone		Diabetic
−463	Clofibrate		Antilipemic
−459	Bis(2-ethylhexyl)phthalate	DEHP	Plasticizer
−458	Thiourea		Agricultural chemical
−447	Cacodylic acid		Agricultural chemical
−446	Amitrole		Agricultural chemical
−445	4-Octylphenol	OP	Reproductive effector
−444	2,6-Dimethylaniline	2,6-Xylidene	Natural product
−443	1,2-Dibromo-3-chloropropane	DBCP	Agricultural chemical
−442	1,1-Dimethylhydrazine	1,1DMH	Reproductive effector
−441	Sulfanylamide		Agricultural chemical
−440	Streptozotocin		Agricultural chemical
−439	Spironolactone		Aldosterone antagonist
−438	*para*-Aminoazobenzene	pAAB	Pigment/mutagenicity/carcinogenicity
−437	*para*-Cresidine		Pigment/carcinogenicity
−436	Neostigmine bromide		Parasympathomimetics
−435	*para*-Dichlorobenzene	pDCB	Pigment/Agricultural chemical
−434	Phenytoin		Antiepileptic
−433	*ortho*-Toluidine	oToluidine	Pigment
−432	Imipramine		Antidepressant
−431	Cobalt chloride		Teratogenicity/mutagenicity
−428	Atrazine		Agricultural chemical
−427	Propylthiouracil		Teratogenicity/carcinogenicity
−426	Thalidomide (L + D)		Teratogenicity
−425	Carbon tetrachloride	CCl_4	Teratogenicity/carcinogenicity
−424	Hydroquinone		Oxidative stress
−423	Monocrotaline		Mutagenicity/carcinogenicity
−422	Vinyl chloride		Carcinogenicity
−421	Tributyltin chloride	TBT	Ship bottom paint/organotin
−420	Valproic acid		Antiepileptic
−419	Benzene		Carcinogenicity